UNIVERSIDADE ESTADUAL DE CAMPINAS
Faculdade de Engenharia Mecânica
Instituto de Geociências

Luciano dos Santos Martins

Productivity Index Map: A New Proposal as Production Potential Sweet Spots

Mapa de Índice de Produtividade: Uma Nova Proposta como Sweet Spot de Potencial Produtivo

CAMPINAS
2024

Luciano dos Santos Martins

Productivity Index Map: A New Proposal as Production Potential Sweet Spots

Mapa de Índice de Produtividade: Uma Nova Proposta como Sweet Spot de Potencial Produtivo

Dissertation presented to the School of Mechanical Engineering and Institute of Geosciences of the University of Campinas in partial fulfillment of the requirements for the degree of Master in Petroleum Sciences and Engineering in the area of Reservoirs and Management.

Dissertação apresentada à Faculdade de Engenharia Mecânica e Instituto de Geociências da Universidade Estadual de Campinas como parte dos requisitos exigidos para obtenção do título de Mestre em Ciência e Engenharia de Petróleo, na área de Reservatório e Gestão

Advisor: Dra. Rosangela Barros Zanoni Lopes Moreno

ESTE TRABALHO CORRESPONDE À VERSÃO FINAL DA DISSERTAÇÃO DEFENDIDA PELO(A) ALUNO(A).. Luciano dos Santos Martins, E ORIENTADA PELO(A) PROF(A). DR(A). Rosangela Barros Zanoni Lopes Moreno

CAMPINAS
2024

Ficha catalográfica
Universidade Estadual de Campinas (UNICAMP)
Biblioteca da Área de Engenharia e Arquitetura
Rose Meire da Silva - CRB 8/5974

Martins, Luciano dos Santos, 1989-
M366p Productivity index map : a new proposal as production potential sweet spots / Luciano dos Santos Martins. – Campinas, SP : [s.n.], 2024.

Orientador: Rosangela Barros Zanoni Lopes Moreno.
Dissertação (mestrado) – Universidade Estadual de Campinas (UNICAMP), Faculdade de Engenharia Mecânica.

1. Simulação de reservatórios. 2. Administração da produção. 3. Planejamento da produção. I. Moreno, Rosangela Barros Zanoni Lopes, 1966-. II. Universidade Estadual de Campinas (UNICAMP). Faculdade de Engenharia Mecânica. III. Título.

Informações Complementares

Título em outro idioma: Mapa de índice de produtividade: uma nova proposta como sweet spot de potencial produtivo
Palavras-chave em inglês:
Reservoir simulation Production management Production planning
Área de concentração: Reservatórios e Gestão **Titulação:** Mestre em Ciências e Engenharia de Petróleo
Banca examinadora:
Rosangela Barros Zanoni Lopes Moreno [Orientador]
Denis José Schiozer
Adolfo Puime Pires
Data de defesa: 24-07-2024
Programa de Pós-Graduação: Ciências e Engenharia de Petróleo

Identificação e informações acadêmicas do(a) aluno(a)
- ORCID do autor: https://orcid.org/0009-0001-2210-034X
- Currículo Lattes do autor: https://lattes.cnpq.br/2031649709645507

UNIVERSIDADE ESTADUAL DE CAMPINAS
FACULDADE DE ENGENHARIA MECÂNICA

DISSERTAÇÃO DE MESTRADO ACADÊMICO

Productivity Index Map: A New Proposal as Production Potential Sweet Spots

Mapa de Índice de Produtividade: Uma Nova Proposta como Sweet Spot de Potencial Produtivo

Author: Luciano dos Santos Martins

Advisor: Prfa. Dra. Rosangela Barros Zanoni Lopes Moreno

A Banca Examinadora composta pelos membros abaixo aprovou esta Dissertação:

Profa. Dra. Rosangela Barros Zanoni Lopes Moreno, Presidente
Departamento de Energia / Faculdade de Engenharia Mecânica / Universidade Estadual de Campinas

Prof. Dr. Denis José Schiozer
Departamento de Energia / Faculdade de Engenharia Mecânica / Universidade Estadual de Campinas

Prof. Dr. Adolfo Puime Pires
Laboratório de Engenharia e Exploração de Petróleo / Universidade Estadual Norte Fluminense

A Ata de Defesa com as respectivas assinaturas dos membros encontra-se no SIGA/Sistema de Fluxo de Dissertação/Tese e na Secretaria do Programa da Unidade.

Campinas, 24 de Julho de 2024.

Dedication

I dedicate this work to my family, who supported and motivated me throughout my master`s degree in Science and Petroleum Engineering.

Acknowledgements

I would like first to thank God to give me this opportunity on the right moment. I also express my gratitude to my family for the support given during the development of this work.

I express my acknowledge to Professor Dr. Rosangela B. Z. L., my advisor, for the opportunity, supervision and belief in my work. Thank you for your patience, teaching and guidance.

I am grateful for the support of CEPETRO students, researchers and technical staff for the good moments and shared knowledge. I would like to give a special thanks to José Maria, Walter Flores and Marx Miranda for the countless and important conversations during this journey

I would also like to thank all the teachers in the subjects in which I enrolled. A special mention to João Carlos Von Hohendorff Filho, who supervised my production strategy optimization project during the reservoir simulation course, and also for all the meetings, patience and conversations.

Finally, I express my appreciation to the Laboratory for Oil Reservoirs (LABORE), School of Mechanical Engineering (FEM), and the State University of Campinas (UNICAMP) for their institutional support.

A special thank you to PETROBRAS for giving me the opportunity and all the necessary conditions to complete this master`s degree.

Resumo

Mapa de qualidade dinâmico é uma representação 2D do reservatório gerado a partir de simulações numéricas. Este é utilizado como ferramenta para auxiliar no posicionamento de poços produtores. Vários métodos foram elaborados para sua construção, adotando a produção acumulada à pressão de fundo constante como índice de qualidade. Esta abordagem tem uma boa correlação com a reserva de hidrocarbonetos, mas não necessariamente captura todos os *sweet spots*, principalmente quando se avalia áreas hidraulicamente desconectadas ou reservatórios distintos. Este estudo tem por objetivo mostrar que o mapa de qualidade baseado no índice de produtividade pode representar melhor o potencial produtivo do poço nos reservatórios.

Através de um modelo analítico sintético homogêneo os resultados para produção acumulada e índice de produtividade foram comparados e submetidos a uma análise de sensibilidade. As simulações de modelos sintéticos heterogêneos extrapolam as observações feitas nas análises anteriores. Os resultados obtidos nesses estudos irão auxiliar a interpretação entre os mapas de qualidade de índice de produtividade e produção acumulada aplicados num modelo benchmark baseado no campo de Namorado em dois cenários distintos. Os mapas de qualidade de índice de produtividade foram construídos a vazão constante e pressões de fundo constante, com valores acima e abaixo da pressão de bolha. Os resultados das anomalias obtidas nestes mapas foram comparados com a posição dos poços produtores numa estratégia de produção otimizada. O efeito de interferência entre poços também foi realizado/estudado/analisado utilizando um modelo analítico multi poços, obtido da literatura, para a obtenção dos valores de índice de produtividade nestas condições. Seus valores foram comparados com os obtidos pelos mapas de indice de produtividade, utilizando as mesmas restrições de poços, que não consideram o efeito de interferência entre poços.

Os resultados dos modelos analíticos e sintéticos mostraram uma dependência da produção acumulada com o volume total de óleo e a diferença entre a pressão inicial do reservatório e a de fundo de poço. Entretando o índice de produtividade pseudo-permanente se mostrou independente a estes parâmetros. Os mapas de qualidade de índice de produtividade foram capazes de correlacionar as anomalias entre blocos hidraulicamente desconectados, independente das condições iniciais do reservatório e operacionais do poço. Uma boa correlação foi observada entre a posição dos poços produtores numa estratégia otimizada e as anomalias obtidas pelo mapa de índice de produtividade, assim como entre os valores de índice de produtividade obtidos levando em consideração a interferência entre poços ou não.

A novidade deste trabalho está na criação do mapa de qualidade baseado no índice de produtividade em que suas anomalias se mostraram invariante as condições iniciais de reservatório e de controle de poço. Seu valor representa a mobilidade efetiva do óleo, que tem relação direta com o potencial produtivo e são similares quando consideramos o efeito de interferência entre poços.

Palavras Chave: Simulação de Reservatório, Mapa de Qualidade, Potencial de Produção, Qualidade de Reservatório, Estratégia de Produção

Abstract

Dynamic quality map is a 2D representation of the reservoir generated from numerical simulations. It is used as a tool to assist in the positioning of producer wells. Several methods have been developed for its construction, adopting cumulative production at constant bottomhole pressure as a quality index. That approach has a good correlation with hydrocarbon reserves but does not necessarily capture the sweet spots, especially when evaluating hydraulically disconnected areas or distinct reservoirs. This study aims to show that the quality map based on the productivity index can represent better the productive potential of the reservoirs.

First, proper definition of the productivity index was reviewed and the relation between cumulative production and productivity index was demonstrated through an analytical model. Then, quality maps considering cumulative production or productivity index as quantity indicators were generated and compare for a synthetic reservoir with two blocks with different permeabilities and for a benchmark model bases on the Namorado Field. Many conditions were tested, including: single-well and multi-well positioning, reservoir at original pressure and depleted reservoir, bottomhole pressure above and below the bubble pressure.

The results of the analytical and synthetic models showed a dependence of cumulative production on the total volume of oil and the difference between the initial reservoir pressure and the bottom well pressure. On the other hand, the pseudo-steady state productivity index proved to be independent of those parameters. The productivity index quality maps were able to correlate anomalies between hydraulically disconnected blocks, regardless of initial reservoir or well operational conditions. A good correlation between the position of the producing wells in an optimized strategy was observed and the anomalies obtained by the productivity index quality map, as well as between the productivity index values obtained taking into account interference between wells or not.

The novelty of this work lies in the creation of the quality map based on the productivity index in which its anomalies proved to be invariant to the initial reservoir or well control conditions. Its value represents the effective mobility of the oil, which is directly related to the productive potential of the reservoir.

Key Word: reservoir simulation, quality map, production potential, reservoir quality, production strategy

LIST OF FIGURES

LIST OF TABLES

LIST OF NOMENCLATURES

Symbols	**Name**	**Unit**
A	= Drainage Area	m2
B	= Formation volume factor	m3 STD / m3
c	= Compressibility	(kgf/cm2)-1
CA	= Shape Factor	dimensionless
D	= Loss Ratio	1/day
h	= Reservoir thickness	m
J	= Productivity Index	(m3/d)/(kgf/cm2)
k	= Reservoir permeability	mD
N	= Oil volume in place surface conditions	m3 STD
Np	= Cumulative production	m3 STD
nprod	= Number of producer wells	dimensionless
p	= Pressure	kgf/cm2
$\bar{p}_D$	= Laplace transformo of dimensionless pressure	dimensionless
q	= Production Rate	m3 STD/d
$\bar{q}_D$	= Laplace transform of dimensionless flow rate	dimensionless
r	= Radius	dimensionless
S	= Saturation	decimal
t	= Time	days
Vp	= Pore volume	m3
wcut	= Water cut	decimal
∂	= Partial derivative	-
μ	= Viscosity	cp
α	= Real positive constant	dimensionless
ϕ	= Porosity	decimal

Subscripts	**Name**
A	Area
avg	Average
b	Bubble point
D	Dimensionless
e	Effective

f	Flowing
i	Initial
max	Maximum
min	Minimum
o	Oil
pss	Pseudo steady-state
t	Total
tot	Total material balance
w	Well
wi	Irreductible water
r	Residual

Constants	**Value**
γ	1.78108

Acronyms	**Name**
BHP	Bottom Hole Pressure
BSW	Basic Sediment and Water
FEI	Field Economic Indicator
FP	Fixed Producers
FPI	Fixed Producers and Injectors
IPR	Inflow Performance Relationship
IWEI	Injector Well Economic Indicator
NPV	Net Present Value
OIIP	Original Oil in Place
OIP	Oil in Place
OWC	Oil Water Contact
PI	Productivity Index
PSS	Pseudo Steady State
PWEI	Producer Well Economic Indicator
RF	Recovery Factor
VOIP	Volume of Oil in Place

Summary

1 INTRODUCTION

The oil field life cycle can be divided into two main phases: Exploration and Production. The first phase starts with wildcats drilling until a new oil discovery is made. The appraisal and delineation stages follow up to gather additional information to determine the extension of the oil reservoir. During these stages, new wells are drilled, and conventional and extended well tests may occur. If the accumulation is economically viable, a declaration of commerciality notification is issued, formally determining the beginning of the production phase. A development strategy is determined aiming of maximizing the income of the field. The main steps involved are the establishment of an initial strategy and the optimization of the number, type, schedule, and position of wells, as well as the platform type and capacity (Gaspar *et al.*, 2016). An objective function is needed to measure the strategy's effectiveness, usually being the net present value (NPV) and the recovery factor (RF). The NPV increases with gross oil volume produced and oil flow rate, because of production anticipation.

Field strategy optimization is a nonlinear problem with no unique solution and several local minimums (Cullick *et al.*, 2005). Gradient-free algorithms are an important class of solutions for this problem, with the counterpart being computationally expensive (Nasrabadi *et al.*, 2012). A common approach to improve optimization performance is to limit the search space of each variable being optimized. An initial solution close to the maximum NPV can also reduce the computational effort. Quality maps are a tool that can assist in both situations (Maschio *et al.*, 2008). This concept was first introduced by Cruz and Horne (1999) as a 2D quality representation of the 3D reservoir model. The maps are generated using the sweep method, simulating one vertical well at a time perforated on all oil layers at each horizontal projection of the grid. A cost-effective proposed solution is to run simulations only in some pints and do a final kriging interpolation. According to the authors, the wells are set to operate under constant bottom-hole pressure (BHP) and a minimum flow rate constrain (q_{min}), with a total time long enough to allow the well to produce all possible oil. Cruz and Horne (1999) are not clear about a specific time range in their work, stating that the same production time must be used to generate the maps if you want to compare reservoirs. The quality index proposed was cumulative production. They developed a large-scale study comparing the quality maps of 50 different reservoir models that were generated using geostatistical tools. As conclusion, they obtained a correlation between the average map quality index and the production potential, allowing to compare different reservoirs and determining good locations for vertical producer wells. Other works followed that development optimizing the map creation speed and suggesting new methodologies for quality map generation, like the application for horizontal wells and the use of fuzzy logic (Nakajima; Schiozer, 2003), multi-well fixed producers and injectors (Cavalcante Filho, 2005), multi-fidelity modeling (Le Ravalec, 2012) and true effective mobility based quality index (Mirzaei-Paiaman; Ghanbarian, 2022).

Whilst the qualitative behavior of the quality maps had been well documented through correlations, it can be noted that none of these integrated an analytical analysis with the results interpretation. Neither of these works also suggested a quality map based on the productivity index.

This work focuses on the development of a new quality map based on the productivity index. This property is constant under the pseudo-steady-state flow regime and its value represents the oil phase mobility, defined as the oil flow rate per unit of pressure drop (Guo *et al.*, 2008). These results will be compared with the traditional cumulative production quality index, with the support of analytical and synthetic models. Finally, a discussion about the single-well and multi-well productivity index will be made. It is expected that the quality map based on the productivity index, as proposed in this work, be directly correlated with the reservoir quality, without dependence on a specific well operational condition.

1.1 Motivation

The motivation of this work is to compare the productive potential among different petroleum reservoir regions and assist in the positioning of producing wells.

1.2 Objectives

The objectives of this work are to generate a quality map based on the productivity index and compare its results with the quality map based on cumulative production, in different scenarios, with the support of analytical and synthetic models.

1.3 Dissertation Structure

This dissertation is composed of six chapters

Chapter 1 presents the Introduction, Motivation and Objectives of this work

Chapter 2 summarizes the theoretical fundamentals of the productivity index and decline curves analysis, that will support the main study of this work. A literature review about quality maps is also presented.

Chapter 3 introduces all methodologies applied in this research. We start from the development of a homogeneous analytical model and simulations of heterogeneous synthetic cases. The next section covers the workflow developed to build the productivity index quality map and the workflow used to build the cumulative production quality map. Finally, we describe the qualitative and quantitative validations methods applied.

Chapter 4 describes the synthetic and real case models simulated using the methodologies presented on Chapter 3.

Chapter 5 shows all results obtained following the methods given in the last chapter. We start with an analytical sensibility analysis and synthetic model results. Then it is presented the quality maps obtained for a real case benchmark model, with a discussion about the differences encountered on each method applied with the support of the analytical and synthetic results. Finally, the validation is applied and compared with the methodology proposed on this work.

Chapter 5 summarizes the main conclusions and future work recommendations.

APPENDIX A is the dimensionless variables definition used in this work

APPENDIX B details each step to obtain the final optimized strategy for the real case

2 LITERATURE REVIEW

This chapter introduces the main concept used to measure well performance on the field, covering subsaturated and saturated reservoirs on Section 2.1. Analytical and empirical models, including field applications that will be used to support and validate this research are covered on Section 2.2. The final topic (Section 2.3) reviews quality map development and applications, which is the main topic of this research.

2.1 Productivity Index

The productivity index (PI) is a way to measure the relative ability of wells to produce. It was first suggested by Moore in 1930 (apud Haider, 1937) being later discussed by Haider in 1937. The objective was to substitute conventional open-flows potential which were expensive because of the surface equipment required to conduct the measurement. Productivity index is defined as the surface flow rate divided by the difference between the reservoir mean pressure and the bottom hole pressure. Its value varies with time during unsteady state, but become constant at pseudo steady state flow regime (Figure 2-1).

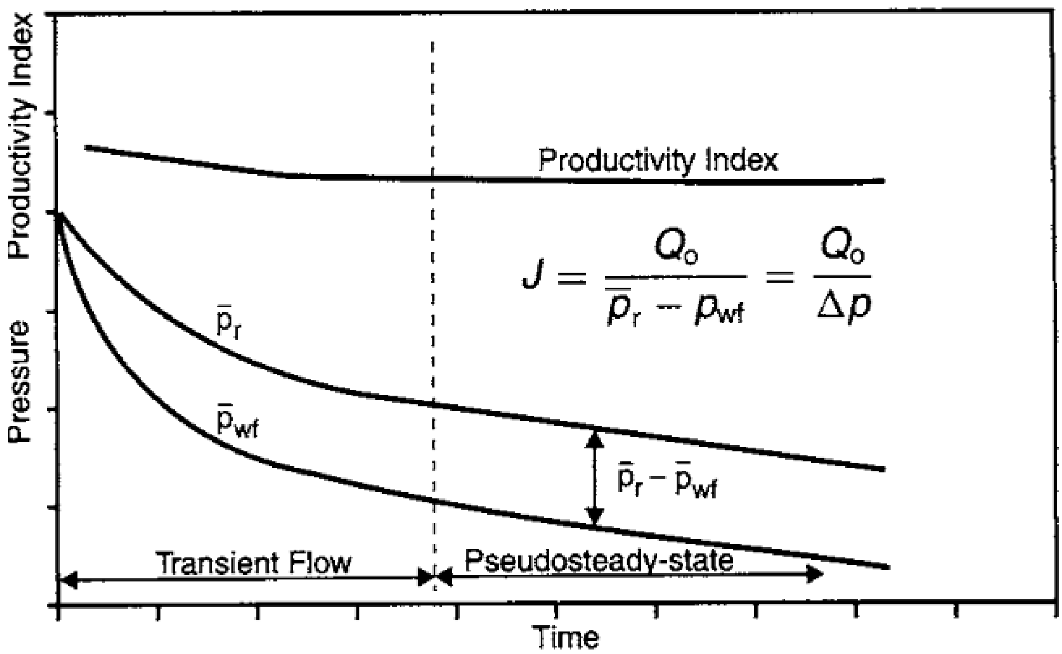

Figure 2-1: Productivity index behavior for different flow regimes. Source: (Ahmed, 2005)

It can be measured on the field by pressure transient tests or production tests. Their difference resides on the producing well constrains, being constant flow rate or constant bottom hole pressure, respectively.

Dietz in 1965 introduced the shape factors (C_A) in order to determine the time needed for a well to reach pseudo-steady state on an arbitrary drainage shape area producing at constant flow rate. This allowed to describe its pressure behavior on these conditions in function of C_A. Helmy in 1998 showed that constant rate and constant pressure shape factors are close in values for regular shapes with centered wells. For irregular shapes, with high width by length ratio and high off-centered wells the difference can increase. Those constants affect the productivity index values at pseudo steady state depending of your well constrains, but in general can be expected to have similar values.

In multiphase flow the PI is not expected to be constant under pseudo-steady state. Its behavior can be observed on a plot of the bottom hole pressure by the flow rate for a specific reservoir mean pressure, denoted as inflow performance relationship (IPR). The PI is proportional to the slope of that plot. Vogel in 1968 developed an empirical model for saturated reservoirs, where he generalized an already known phenomena showed by Muskat (1946), that is the quadratic fall of oil production performance due to well bottom hole or reservoir pressure below the bubble point (Pb), as showed on Figure 2-2.

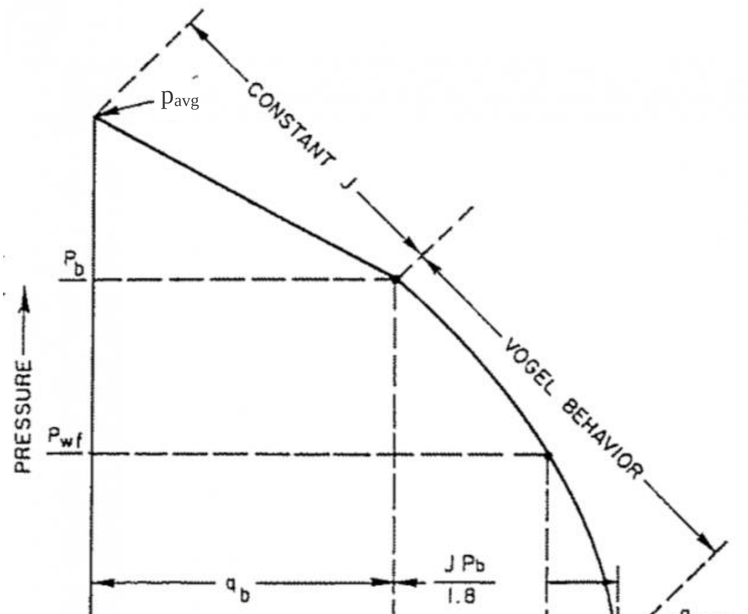

Figure 2-2: Empirical pseudo steady state PI behavior for subsaturated and saturated oil reservoirs for different pwf's. Source: (Vogel IPR, 2024)

2.2 Decline curve analysis

Decline curve analysis is an empirical mathematical model to forecast wellbore behavior based on field data. It was categorized by Arps (1945) using the loss ratio, defined as the inverse of the percentual flow rate decay over time (-q/(dq/dt)). There are three main curve decline types, illustrated in Figure 2-3, depending on the time derivative of the loss ratio (b): harmonic (b = 1), hyperbolic (1 >= b > 0) and exponential (b = 0).

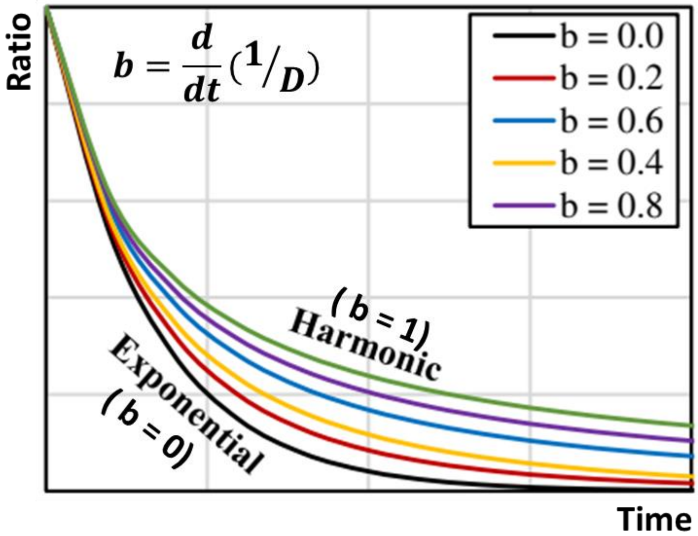

Figure 2-3: Arps Decline type curves. Source: Modified from Wood and Cai (2021)

It was later shown by Fetkovich (1980) that the exponential decay has an analytical solution for a single well producing at constant bottom hole pressure at pseudo steady state. This decline behavior was also presented on a multiwell system, first introduced by Rodriguez and Cinco-Ley (1993) apud Marhaendrajana and Blasingame (2001) for wells producing at constant bottom hole pressure at pseudo-steady state. Later it was generalized for any flow regime and rate/pressure profile through analytical model, synthetic simulation and real case application (Marhaendrajana; Blasingame, 2001). They validated the generalized model by using homogeneous and heterogeneous synthetic cases and a real case application. Their primary objective was to determine the original volume of hydrocarbon in place based on type curves using a multiwell analysis as a function of the material balance time.

2.3 Quality Maps

The concept of quality map was first introduced by Cruz and Horne (1999). Their objective was to develop a 2D representation of the 3D simulation model to assist on the positioning of producer wells. The map was built it using the sweep method, running several flow simulations with a single vertical well perforated on all oil layers, varying its location on each run. The well was constrained by a minimum bottom hole pressure and a minimum flow rate, without maximum flow rate restrictions. The production time needed to be long enough to allow to produce all possible oil. The quality index used to represent the cell values was the cumulative production (N_p). They also showed that the mean value of the quality index could be used to rank reserves of new reservoirs as long as the same well controls and times of production were used when generating the maps (see Figure 2-4).

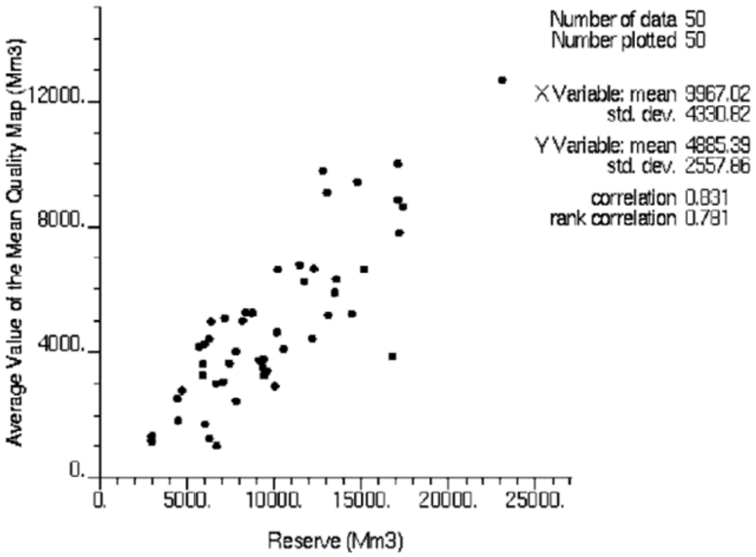

Figure 2-4: Linear correlation between average value of the quality map (cumulative production) and reservoir reserves. Source: (Cruz; Horne, 1999)

Nakajima And Schiozer (2003) compared three methodologies of quality maps generation focused on horizontal wells. The first methodology was based on numerical simulation of a group of fixed horizontal wells opened at the same time on each layer of the model. The final map was given by the average of the cumulative oil production on each well in all layers. The second methodology was based on Babu And Odeh (1989) analytical model for horizontal wells. That was applied to a reservoir modeled as a box-shaped drainage volume of an arbitrary size. The last quality map was generated considering a fuzzy system method with classification rules based on static reservoir properties. The output is a real value between 0 and 1, which represented the reservoir quality. Their objective was to test which map had the best correspondence with well performance, correlating the quality values obtained with the Net Present Value (NPV) of an optimized strategy on a modified campos basin reservoir. They found that the fuzzy map provided the best results with the highest correlation. This method don`t require computational models, but need a variable input list and a quality discrete classification of the input and output based on the knowledge and experience of specialists.

Cavalcante Filho (2005) adapted the Cruz and Horne (1999) method to speed up the vertical well quality map generation. He proposed fixed producers (FP) and fixed producers and injectors (FPI) maps using a well pattern configuration. Using that, the respective maps are generated in a unique simulation run. However, according to the authors, the user needs to input calibrations to get reliable results. To avoid that, in their approach, all wells operate under the applied constrains during the entire simulation time. The final map is obtained by kriging the values between the producer wells. His study was applied in synthetic and real case models, and the results were compared with Cruz and Horne (1999) full-sweep method. According to Cavalcante Filho (2005), the FPI method showed more consistent results.

Quality maps were also used to determine the best infill well locations on mature fields optimization studies (Cottini-Loureiro and Araujo, 2005). Le Ravalec (2012) developed a faster processing for a full map obtaining, using data from models with different resolutions. Recent works opened the discussion for other quality indexes besides the cumulative production, based on the true effective mobility of rocks (Mirzaei-Paiaman and Ghanbarian, 2022).

3 METHODOLOGIES

The investigation of this work can be divided into three main parts: 1) the development of an analytical model to understand the relationship between cumulative production and productivity index, 2) the simulation of a synthetic model to validate the observations made in the previous step in a more general approach, and 3) the application of the cumulative production and productivity index map on a benchmark case. The workflow used in this work is represented in Figure 3-1 and is described below.

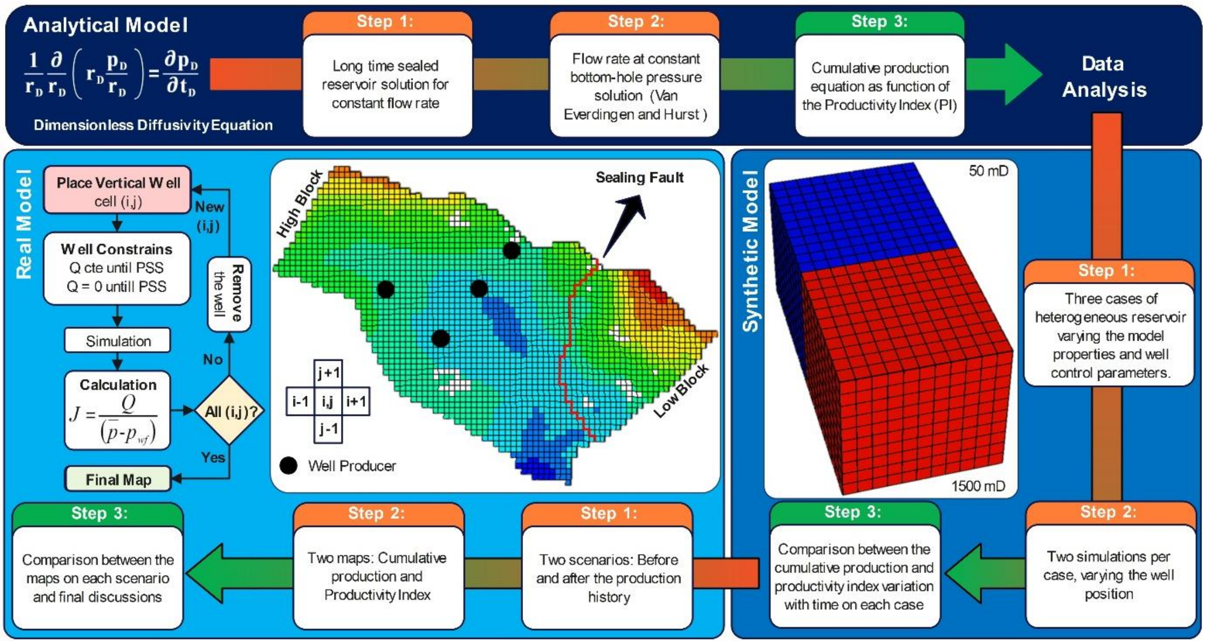

Figure 3-1: Productivity Index Maps Validation Workflow: Analytical model, Synthetic Simulation and a Real Case Application

Each of those studied parts can be subdivided into three main steps as stated in Figure 3-1. The analytical model analysis (Part 1) starts from the classical radial diffusivity equation to obtain the cumulative production as a function of the productivity index under constant bottom-hole pressure constrained by a minimum flow rate. This model is going to be used to understand how the cumulative production varies with the pseudo-steady state productivity index through a sensitivity analysis.

The second part, based on synthetic simulation models, are used to analyze the effect of distinct productivity index on the cumulative production for different well positions on the same reservoir. These results are compared on Section 5.1 with the analytical model obtained on Section 3.1.1 and they give support to the real case maps interpretation.

Part 3 consists of the application of the productivity index map, as suggested by this research. The cumulative production map, proposed by Cruz and Horne (1999), will be used as reference. The results are derived considering a real benchmark case based on the Namorado Field (Gaspar *et al.*, 2023a), where two scenarios were chosen to test the quality maps.

Finally, a validation of the productivity index map will be made. Qualitatively, the results will be compared with an vertical well optimized production strategy. Quantitatively, the PI map values will be compared with those obtained by a multi-well model proposed by Marhaendrajana and Blasingame, 2001. More detailed information about the methodologies will be provided in the next topics of this chapter.

3.1 Support Models for Results/Quality Maps Interpretation

On this topic we show the derivation of an analytical model of the cumulative production under constant bottom hole pressure in function of the productivity index (Section 3.1.1). This model is used in chapter 5 to identify the main variables affecting the cumulative production through a sensitivity analysis. Synthetic simulations will also be made to expand the observations made by the analytical model to heterogeneous reservoirs. The methodology used on each model presented on Section 4.1 is described on Section 3.1.2. The final results and discussions are presented on Chapter 5.

3.1.1 Homogeneous Analytical Case

We start from the single-phase flow dimensionless radial diffusivity equation:

$$\frac{1}{r_D}\frac{\partial}{\partial r_D}\left(r_D\frac{p_D}{r_D}\right)=\frac{\partial p_D}{\partial t_D} \tag{EQ1}$$

It's solution for a sealed reservoir of arbitrary shape producing at constant flow rate is well known. Taking it`s long time approximation (Lee *et al.*, 2003), and using the definition of $J_{Dpss}=J_{pss}\frac{B_o\mu_o}{2\pi k_o h}$ (Diyashev; Economides, 2006), we have:

$$p_D(t_{DA})=2\pi t_{DA}+{}^{1}\!/_{J_{Dpss}} \tag{EQ2}$$

Taking the Laplace transform of EQ2 we get:

$$\mathcal{L}\{p_D\} = \frac{2\pi}{u^2} + \frac{1}{u}\frac{1}{J_{Dpss}} \qquad \text{(EQ3)}$$

The constant bottom hole pressure solution can be obtained with the constant flow rate solution at the Laplace space. Using the Van Everdingen and Hurst (1949) relation ($\bar{q}_D = \frac{1}{u^2 \bar{p}_D}$) on EQ3 we have that:

$$\bar{q}_D = J_{Dpss} / \left(2\pi J_{Dpss} + u\right) \qquad \text{(EQ4)}$$

Taking the inverse Laplace transform of EQ4,

$$\mathcal{L}^{-1}\{\bar{q}_D\} = J_{Dpss} e^{-2\pi J_{Dpss} t_{DA}} \qquad \text{(EQ5)}$$

Putting EQ5 in dimension variables using the relations presented on Appendix A, results:

$$q(t) = J_{pss}(p_i - p_{wf}) e^{-\frac{J_{PSS} B_o}{c_{eo} N B_{oi}} t} \qquad \text{(EQ6)}$$

We can note as stated on Section 2.2 that EQ6 is an analytical model of the exponential decline. The cumulative production can be obtained integrating EQ6 from zero to time t, where t > t_{pss}.

$$N_p(t) = \frac{N B_{oi} c_{eo} (p_i - p_{wf})}{B_o} \left(1 - e^{-\frac{J_{PSS} B_o}{c_{eo} N B_{oi}} t}\right) \qquad \text{(EQ7)}$$

Studying the limits of EQ7, and considering high exponent values the exponential term is neglectable, giving a constant maximum primary production dependent of the oil in place, effective oil compressibility and the pressure difference between the reservoir and the well as showed in EQ8.

$$\frac{J_{PSS} B_o}{c_{eo} N B_{oi}} t \gg 1\, ;\; N_p(t) \approx c_{eo} N B_{oi} (p_i - p_{wf}) / B_o \qquad \text{(EQ8)}$$

For low exponent values we have that $e^{-x} \approx 1 - x$. That makes the cumulative production being directly proportional to the pseudo steady-state productivity index multiplied by the pressure difference, that is the flow rate, as stated below:

$$\frac{J_{PSS}B_o}{c_{eo}NB_{oi}}t \ll 1 \; ; \; N_p(t) \approx J_{PSS}(p_i - p_{wf})t \qquad \text{(EQ9)}$$

For an intermediate case, we suppose a production until a minimum flow rate (q_{min}) is reached, as proposed by Cruz and Horne (1999). From EQ6, assuming a t_{min} is the time necessary to reach q_{min} we have:

$$e^{-\frac{J_{PSS}B_o}{c_{eo}NB_{oi}}t_{min}} = \frac{q_{min}}{J_{pss}(p_i - p_{wf})} \qquad \text{(EQ10)}$$

Substituting EQ10 on EQ7 we finally have the cumulative production until a minimum flow rate is reached.

$$N_p = \frac{NB_{0i}c_{eo}(p_i - p_{wf})}{B_0}\left[1 - \frac{q_{min}}{\boldsymbol{J_{pss}}(p_i - p_{wf})}\right] \qquad \text{(EQ11)}$$

This model is going to be used to understand how the cumulative production varies with the pseudo-steady state productivity index. It's important to note that this relationship is valid under the following reservoir assumptions:

- Undersaturated with an arbitrary area shape
- Homogeneous and Isotropic
- Radial single phase flow and pseudo-steady-state (pss) flow
- Full penetrating vertical well at constant bottom-hole pressure
- Production until it reaches a minimum flow rate

3.1.2 Heterogeneous Synthetic Simulation

Simulations were done using CMG software and Peaceman well model on a synthetic rectangular heterogeneous reservoir model as showed on Figure 3-2. Three cases are studied and detailed on Section 4.1 Synthetic Case Models Description, where the oil volume and well constrains vary between them. On each case two simulations are done, with one vertical well perforated in all layers and producing at constant bottom hole pressure. The pseudo steady-state productivity index of each well are obtained using the same methodology presented on Section

3.2.1 Productivity Index Quality Map Generation. Comparison of the cumulative production history is done among the simulations and the final results are compared with the analytical one.

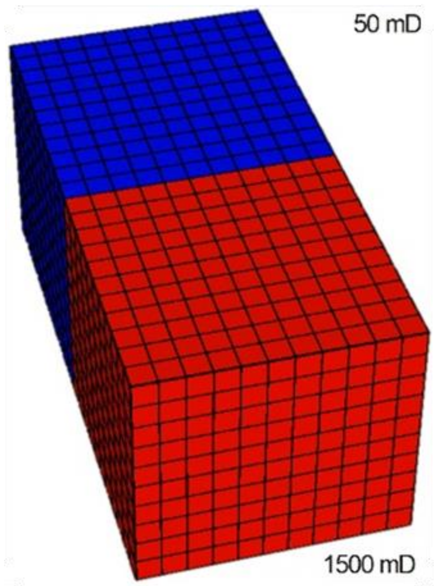

Figure 3-2: Heterogeneous Synthetic Model

3.2 Quality Maps

On this topic, we describe the methodologies used to generate the quality maps that will be applied on the real case model, detailed on Section 4.2 Real Case Model Description. They were generated using the CMG software with Peaceman well model. The productivity index quality map workflow, that is the main proposal of this research, is presented on Section 3.2.1. Finally, a reference quality map workflow based on the cumulative production (Cruz; Horne, 1999) is shown, with the comparisons that will be made between those methods (Section 3.2.2).

3.2.1 Productivity Index Quality Map Generation

The workflow applied to build the productivity index quality map follows similar procedures applied by Cruz and Horne (1999). Several simulations were done, placing one single vertical well perforated on all oil layers on each horizontal cell for each run (Figure 3-3).

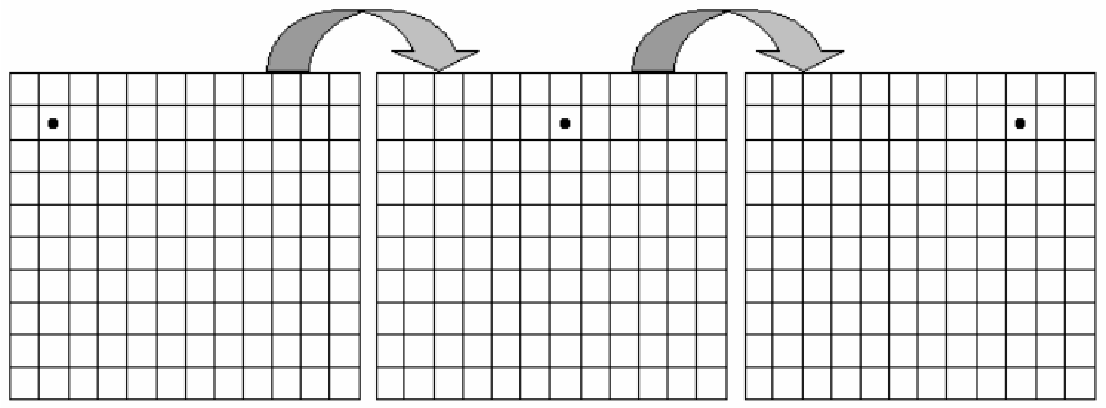

Figure 3-3: Schematic example of well position variation for quality map generation. Source: Cavalcante Filho, 2005

The main differences are on the well constrains. For the PI map, we set the well production at a constant flow rate or constant bottom hole pressure until pseudo-steady state flow condition is reached and close the well immediately after, allowing a build-up pressure. The productivity index is calculated by the ratio between the flow rate and the difference between the reservoir mean pressure and the well bottom hole pressure. Figure 3-4a shows this workflow in detail and Figure 3-4b is a practical example of two distinct well positions under constant flow rate.

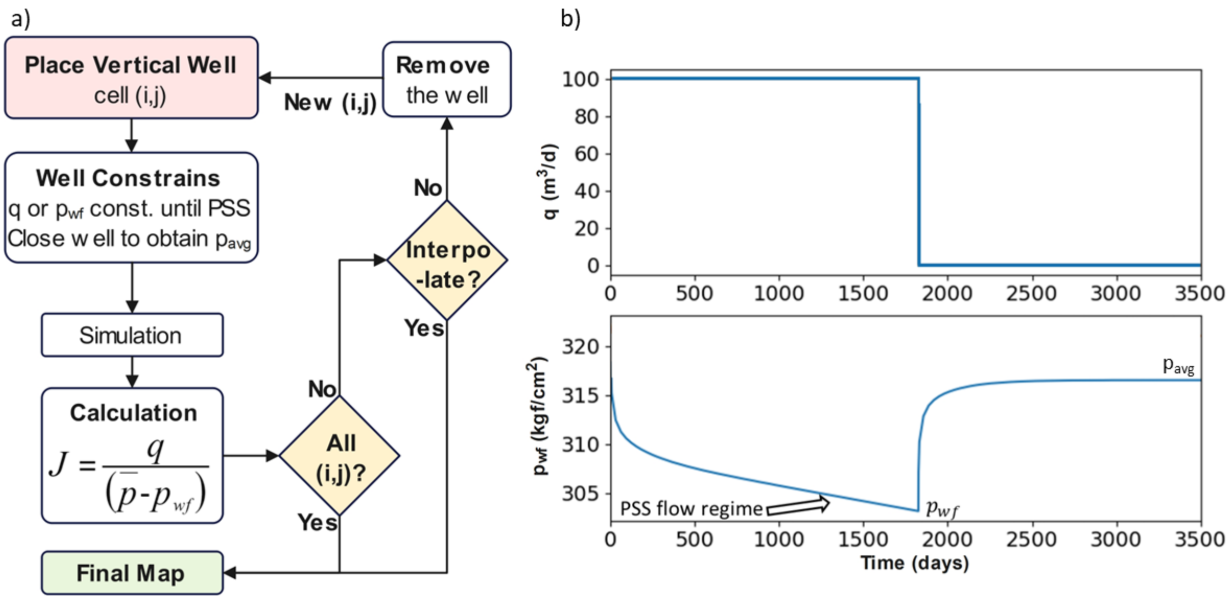

Figure 3-4: Productivity index quality map a) general workflow and b) practical example

The mean reservoir pressure is taken from the final build up, and the bottom hole pressure used is the value right before the well is closed. Constant bottom-hole pressure constrain follows a similar procedure. The final map presented in this work was obtained without the use of spatial interpolation. The wells were completed in all oil layers, 30m above the OWC.

3.2.2 Reference Methodology and Comparisons

The reference method used to compare the results obtained by the productivity index map was the cumulative production quality map proposed by Cruz and Horne (1999). Several simulations were done varying the horizontal position of a vertical well perforated on all oil layers, like showed on Figure 3-3. The wells don't have a limit flow rate and are constrained to operate with a minimum bottom hole pressure. They also are closed if a minimum flow rate or a maximum BSW is reached. Figure 3-5 contains the cumulative production quality map workflow used in this work.

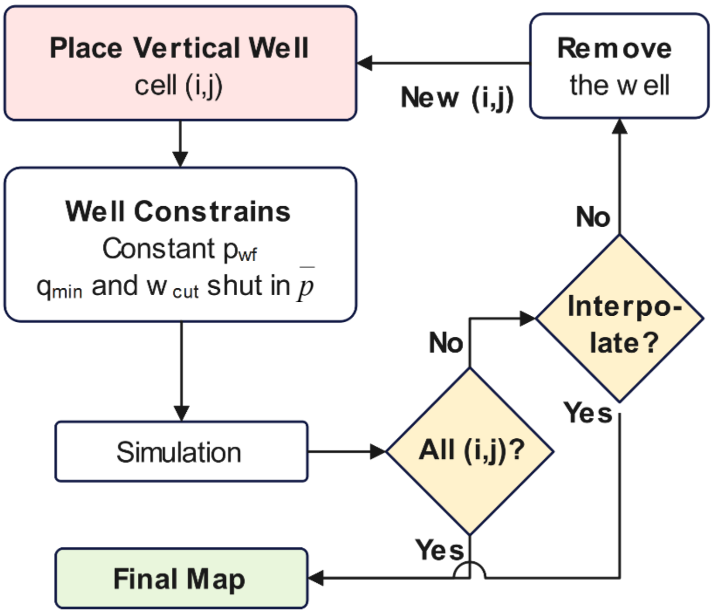

Figure 3-5: Cumulative production quality map workflow generation used in this work

According to Cruz and Horne 1999, the total time of production must be long enough to allow the well to produce all possible oil, given the operational controls of the well. Also, they orient to use the same production time if we want to compare different reservoirs. Taking these rules into account, we simulated each well of each scenario for 26 years, that is the total project time. The maps presented in this work were simulated on all horizontal cells, having no need to do spatial interpolation. The wells were completed on all oil layers, 30m above the OWC. They were set to operate at a constant bottom hole pressure of 190 kgf/cm^2, following the real case model benchmark guide (Gaspar *et al.*, 2023b). These maps are directly compared with the ones obtained on Section 3.2.1, and a cross plot between their values will be made.

3.3 Validation

To validate the productivity index quality map we propose a qualitative comparison with a vertical well optimized strategy. The first topic (Section 3.3.1) summarizes the steps to reach the final strategy. Detailed information about the development to obtain it is in Appendix B. A quantitative approach was also performed, where an analytical multi-well model proposed by Marhaendrajana and Blasingame (2001) was used to calculate the productivity index of each well on a multi-well system (Section 3.3.2). On Chapter 4, those values will be compared with the ones obtained for the productivity index quality map, which represents a single well system. That is crucial to analyze the effects of well interference in PI. On Section 3.3.3, we show how we addressed the sensitivity analysis of the productivity index variation with the drainage area size.

3.3.1 Vertical Well Optimized Strategy

First a history match was done using the production history of the already drilled wells, varying the rock compressibility and the relative permeability curves. The adjusted model was used to develop our production strategy. The workflow followed a hierarchical approach suggest by Gaspar *et al.* (2016), as showed on Figure 3-6.

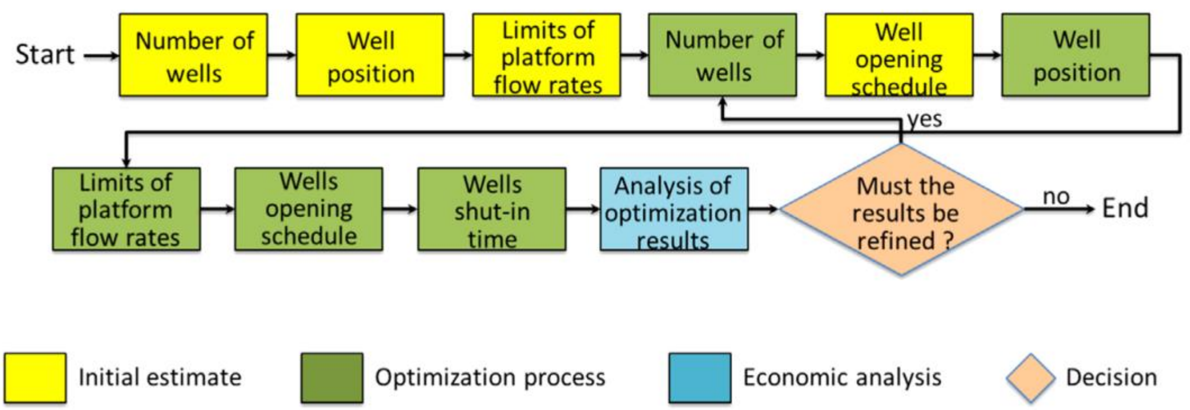

Figure 3-6: Hierarchical field strategy optimization. Source: (GASPAR, Ana Teresa F.S.; BARRETO; SCHIOZER, 2016)

The initial strategy starts by defining the number and positions of wells, all of them opening at the same time, with no flow restrictions by the platform. Net Present Value (NPV) was defined as the objective function, and all the economic parameters were taken from the benchmark manual. An optimization of the number of wells was carried out, immediately defining an initial opening schedule for production wells based on their Producer Well Economic Indicator (PWEI), and alternating the opening of neighboring injectors. The well positions were optimized using a methodology developed by the author. Basically, it was defined a limited search region for each well and their position were optimized one at a time. Optimal values of platform limit were based on a percentage of a standard defined limit. Well opening schedules scenarios were built, and the best one was picked up. Shut-in times were based on the Basic Sediment and Water (BSW) percentage.

Detailed information of the steps taken to reach the final strategy are on Appendix B. The strategy obtained will be compared with other ones from the literature and will be used to qualitatively validate our productivity index quality map.

3.3.2 Well Productivity Index in a Multi Well System

When a production strategy is implemented, we have a multi-well system. Then we need an approach to calculate the individual wells PI s on a multi-well system. Marhaendrajana and Blasingame (2001) proposed an analytical multi-well model to determine the original hydrocarbon in place of a reservoir. Their methodology was tested on homogenous and heterogeneous synthetic models, being finally validated for a real field application. Their equation is showed below:

$$\frac{(p_i - p_{wf,k}(t))}{q_k(t)} = \frac{1}{Nc_t}\bar{t}_{tot} + f(t) \qquad \text{(EQ12)}$$

where $\bar{t}_{tot}$ is the total material balance time, defined as:

$$\bar{t}_{tot} = \frac{1}{q_k(t)}\int_0^t q_i(\tau)d\tau = \frac{N_{p,tot}}{q_k(t)} \qquad \text{(EQ13)}$$

The authors correlated EQ12 with the boundary dominated flow solution for a single well to define $f(t) \equiv b_{pss,mw}$ which is denominated as a “constant in the pseudo-steady-state equation for liquid flow” (Doublet *et al.*, 1994), but in a multi-well system. We will show that this constant is proportional to the productivity index. Starting from the undersaturated material balance equation, and assuming $B_o = B_{oi}$ we have:

$$N = \frac{N_p}{(p_i - \bar{p})c_t} \to \bar{p} = p_i - \frac{N_p}{Nc_t} \quad \text{(EQ14)}$$

Taking the productivity index definition we get:

$$J(t) = \frac{q}{\bar{p}(t) - p_{wf}(t)} \to \bar{p} - p_{wf} = \frac{q}{J(t)} \quad \text{(EQ15)}$$

Substituting the mean pressure of EQ14 into EQ15 we finally get:

$$\frac{(p_i - p_{wf})}{q} = \frac{1}{Nc_t} t_{tot} + \frac{1}{J(t)} \quad \text{(EQ16)}$$

Correlating EQ16 with EQ12 we have that f(t) is equivalent to the inverse of the productivity index. Knowing that, a workflow to calculate the pseudo-steady state productivity index on a multi-well system is shown on Figure 3-7.

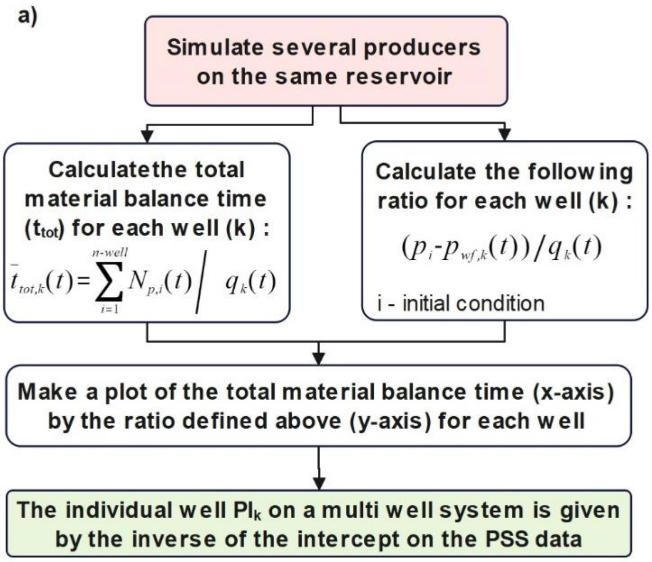

Figure 3-7: Method used to calculate individual well PI on a multi-well system

We start simulating several producers in the same reservoir, for a time long enough to reach and bypass the pseudo-steady state flow regime for all wells. We plot the material balance time for each well on the x-axis and on the y-axis, we plot the difference between the initial pressure and the specific well bottom-hole pressure, divided by the flow rate. Its important to note that this ratio is not the productivity index because, in this case, the initial pressure is used instead of the mean pressure. According to EQ12 its expected a straight line behavior for the pseudo-steady state. A practical example for a specific well is shown on Figure 3-8.

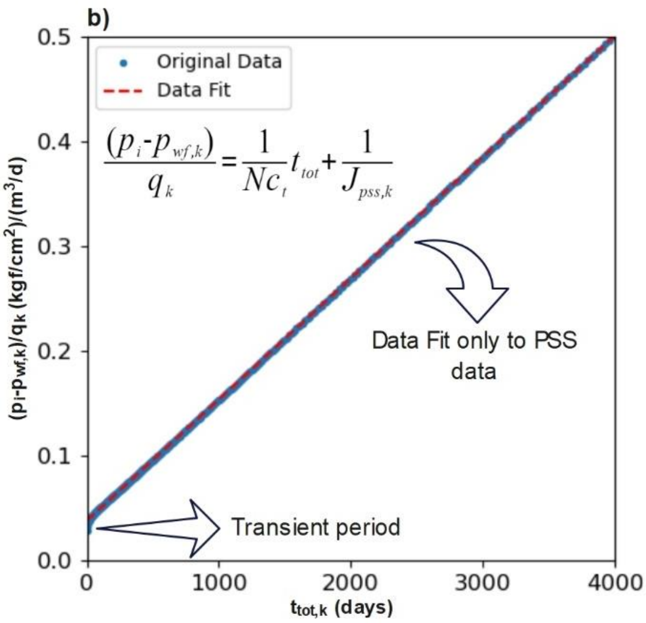

Figure 3-8:Practical calculation of the individual well pseudo-steady state PI on a multi well system.

We can note a transient period on early time, but a linear behavior is seen shortly after. The productivity index is calculated as the inverse of the intercept on the pseudo-steady state data.

3.3.3 Productivity Index Variation with Drainage Area

To do a sensibility analysis of the influence of the drainage area on the productivity index, we start from its definition in the pseudo-steady state flow regime given by the EQ17.

$$J_{pss} = \frac{2\pi k_o h}{B_o \mu_o \frac{1}{2} ln \frac{4A}{\gamma C_A r_w^2}} \qquad \text{(EQ17)}$$

If we assume that A_1 is the total area of the reservoir and $A_2 = A_1/\alpha$ ($\alpha \geq 1$) is the new drainage area in a multi-well system, we can determine the drainage area effect on well interference in the pseudo-steady state productivity index by calculating the ratio of J_{pss1}/J_{pss2}, given by the following equation:

$$\frac{J_{pss1}}{J_{pss2}} = \frac{ln \frac{4A_2}{\gamma C_A r_w^2}}{ln \frac{4A_1}{\gamma C_A r_w^2}} \xrightarrow{yields} \frac{J_{pss1}}{J_{pss2}} = 1 - \frac{ln\alpha}{ln \frac{4A_1}{\gamma C_A r_w^2}} \qquad \text{(EQ18)}$$

EQ18 is used in the next chapter to do a sensibility analysis of this ratio, J_{pss1}/J_{pss2} varying the drainage area size and the well position relative to the area by changing alpha (α) and the shape factor C_A respectively.

4 APPLICATIONS

In this chapter, we describe all the heterogeneous synthetic simulated models, in order to extrapolate the observations made for the homogeneous analytical model. The benchmark case model based on Namorado Field is also introduced with the scenarios used to build the quality maps.

4.1 Synthetic Case Models Description

On this topic we describe the heterogeneous synthetic models used to evaluate and compare the quality maps based on productivity index and cumulative oil production. Three cases were done, being Case A (Section 4.1.1) the default scenario. Case B (Section 4.1.2) was run considering 50% of the Case A porosity value and Case C (Section 4.1.3) was simulated considering 50% of the Case A pressure difference. All these cases were evaluated aiming to extrapolate the observations made for the homogeneous analytical model to heterogeneous reservoirs. The productivity index of each simulated well was calculated using the methodology presented on Section 3.2.1. The results and discussions is presented on Chapter 5.

4.1.1 Heterogeneous Synthetic Case A

The heterogeneous synthetic Case A is a rectangular model of dimensions (x,y,z) equal 100m x 200m x 100m. It is isotropic with a porosity of 20% for the hole grid and the permeability is 1500 mD for the lower half and 50 mD for the upper half as illustrated in Figure 4-1. Two simulations were run, each one having one vertical well perforated on all layers at the 1500md block (Figure 4-1a) or at the 50 mD block (Figure 4-1b).

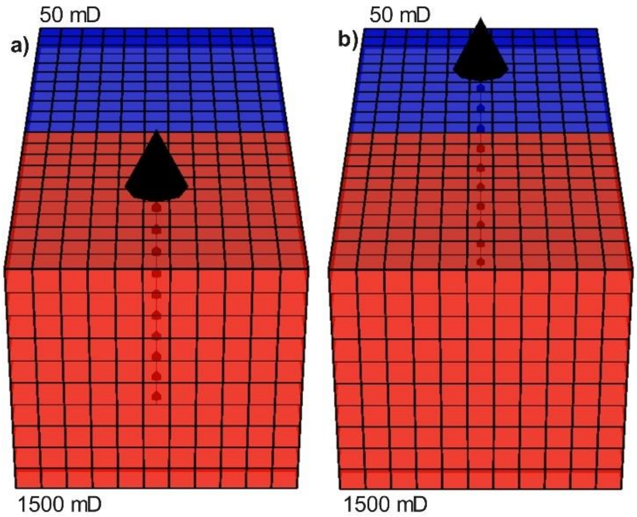

Figure 4-1 Rectangular synthetic model used in this study. a) well perforated on the 50 mD block and b) well perforated on the 1500 mD block

The well was constrained to produce at a constant bottom hole pressure of 300 kgf/cm^2. The rock and fluid properties that remained constant in the synthetic models are summarized on Table 4.1**Erro! Fonte de referência não encontrada.**.

Table 4-1: Synthetic Model Constant Properties

r_w	ϕ	c_o	c_f @ 322kgf/cm^2	μ_o	K_{ro}	p_i	p_b
8.4 in	20%	1.62 e-4 1/kgf/cm^2	53.0 E-6 1/kgf/cm^2	1 cp	1	327 kgf/cm^2	210 Kgf/cm^2

4.1.2 Heterogeneous Synthetic Case B

This model has the same dimensions and properties of Case A. The only difference is that the porosity is 10% for the whole model instead of 20%. Two simulations were also done, as illustrated on Figure 4-1, with the same well constrains of Case A. The synthetic simulations results are compared with the analytical model and the real case results.

4.1.3 Heterogeneous Synthetic Case C

This model has the same dimensions and properties of Case A. Two simulations were also done, as illustrated on Figure 4-1. The well constrains were changed to produce at a constant bottom hole pressure of 313.5 kgf/cm^2. That makes the pressure difference $\left(p_i - p_{wf}\right)$ of Case C half of Case A and Case B. The synthetic simulations results are compared with the analytical model and the real case results.

4.2 Real Case Model Description

The methods, detailed on Section 3.2.1 and Section 3.2.2 for quality maps obtaining, were applied to UNISIM-I-D simulation model (Avansi; Schiozer, 2015). This benchmark is public domain and based on Namorado field. It is an undersaturated oil sandstone reservoir with a sealing fault dividing it into two main blocks, the high block and the low block, as illustrated in Figure 4-2.

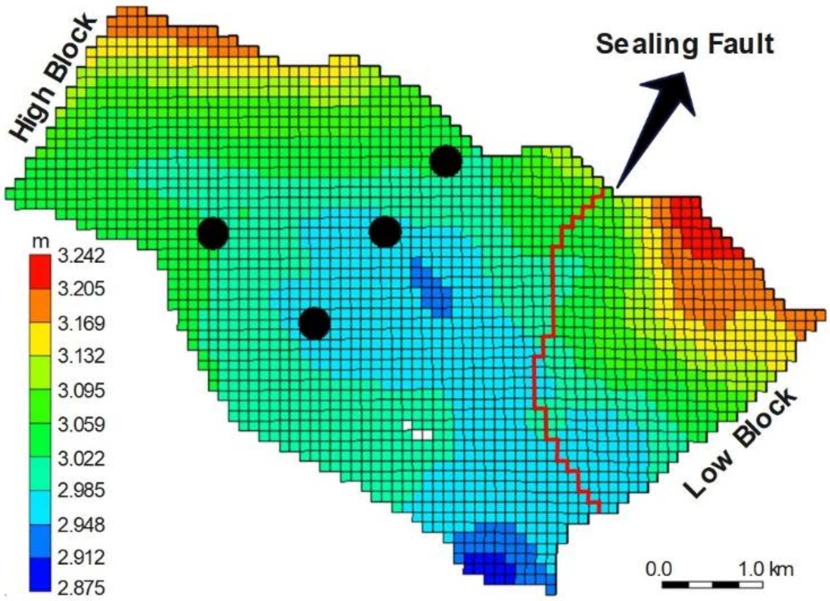

Figure 4-2: Namorado field top structure elevation in meters. The two blocks are hydraulic disconnected by a sealing fault.

Two scenarios were chosen to test the quality maps, one considering the entire reservoir at its original pressure, and the other for the high block depleted due to the production history of four producer wells already drilled. The pressure map for each case is shown in Figure 4-2, with the average pressure, total oil production and oil in place for each block displayed in Table 4-2.

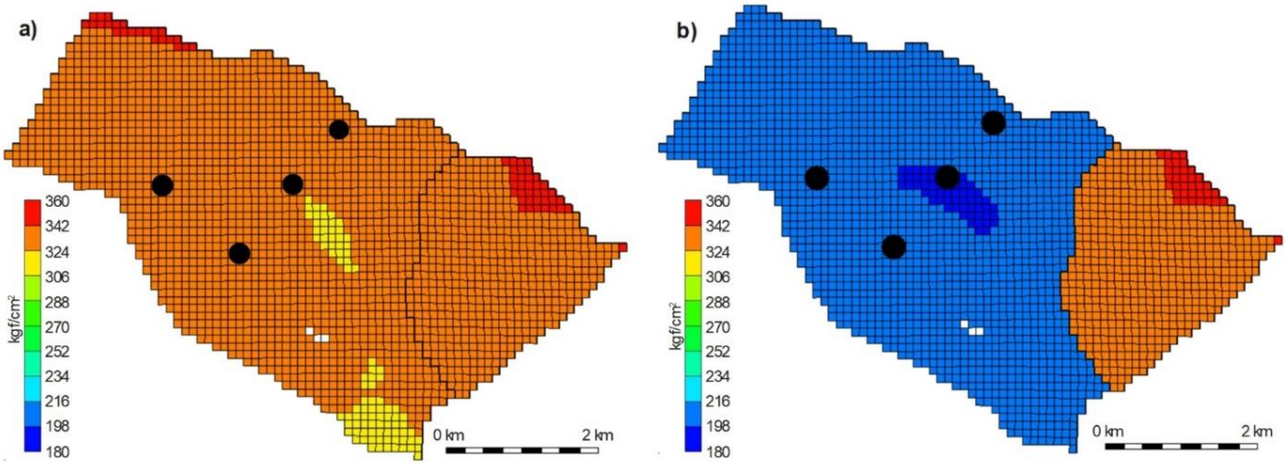

Figure 4-3: Initial reservoir pressure condition for each scenario. (a) High and Low block pavg = 330 kgf/cm2 ; (b) High block pavg = 205 kgf/cm2 and Low block pavg = 330 kgf/cm2.

Table 4-2: Main properties for each scenario of Namorado Field Benchmark

	Case a)			Case b)		
Block	P_{avg} (kgf/cm2)	OIP (MM m3)	Np (MM m3)	P_{avg} (kgf/cm2)	OIP (MM m3)	Np (MM m3)
High Block	330	138.4	0	205	134.3	4.1
Low Block	330	41.1	0	330	41.1	0

According to the benchmark deterministic study case (Gaspar *et al.*, 2023b) the project has 26 years of production after 4 years of production history. Those scenarios were chosen in order to show the quality maps variation with reservoir properties.

5 RESULTS AND DISCUSSIONS

This chapter presents the results of the methods applied to generate Quality Maps. It starts describing the productivity index effects on cumulative production through an analytical sensitivity analysis and synthetic model simulations (Section 5.1). Then the productivity index map is applied to a real benchmark case based on Namorado field (Avansi; Schiozer, 2015) and compared with the cumulative production quality map proposed by Cruz and Horne (1999) (Section 5.2). Finally, on Section 5.3, a qualitative validation is made comparing the productivity index map with the well positions of an optimized strategy presented on Section 3.3.1 and detailed in Appendix B. A quantitative validation is also done by comparing the map values with those obtained from an analytical multi-well model proposed by Marhaendrajana and Blasingame (2001). A discussion will be made on each topic about the results obtained.

5.1 Productivity Index Effects on Cumulative Production

The results of the analytical and synthetic models introduced on Section 3.1 are shown below.

5.1.1 Sensitivity Analysis with Analytical Model

Starting from EQ11 obtained on Section 3.1.1, we will analyze the influence of the productivity index on the cumulative oil production. Assuming two distinct homogeneous reservoirs with the same oil volume in place (NB_{oi}), formation volume factor (Bo), effective oil compressibility (c_{eo}) and pressure difference ($p_i - p_{wf}$), but with distinct pseudo-steady state productivity indexes (J_{pss1} and J_{pss2}), their cumulative production ratio is given by the equation below:

$$\frac{N_{p1}}{N_{p2}} = \frac{1 - \dfrac{q_{min}}{J_{pss1}(p_i - p_{wf})}}{1 - \dfrac{q_{min}}{J_{pss2}(p_i - p_{wf})}} \qquad \text{(EQ19)}$$

The minimum flow rate (q_{min}) used was 20 m^3/d and the pressure difference (p_i-p_{wf}) was 140 kgf/cm^2. Those values are in accordance with the benchmark model (Avansi; Schiozer, 2015) and manual for the study case presented by Gaspar *et al.* (2023b). Typical conventional reservoir values of productivity index were used for J_{pss2}, ranging from 1 to 100 $(m^3/d)/(kgf/cm^2)$, which can be found in the literature (Weimer, 2000), (Warszawski and Ferreira, 2011) and (Warszawski and Ferreira, 2013). Figure 5-1 is a 2D plot of the ratio given by EQ19. The color scale is the cumulative production ratio (N_{p1}/N_{p2}) with constant values represented by contour lines. The x-axis is the J_{pss} ratio (J_{pss1}/J_{pss2}), with $J_{pss1} \geq J_{pss2}$, and y-axis is J_{pss2}.

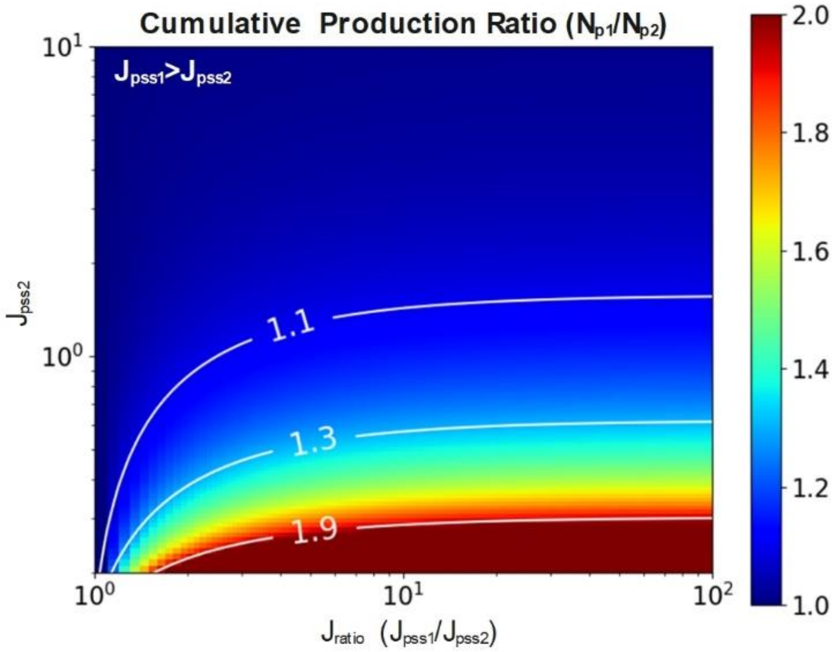

Figure 5-1: Comparison between the productivity index ratio (x-axis) with the Cumulative production ratio (colorscale)

The plot above shows that the productivity index ratio has a low impact on the cumulative production ratio for J_{pss2} values higher than 1 (m^3/d)/(kgf/cm^2). The cumulative production ratio variation tends to stagnate while the J_{pss} ratio ranges from 1 to 100. Those results highlight that the main factor controlling the N_p values, when comparing different reservoirs, is the product $N.c_{eo}.(p_i\text{-}p_{wf})/B_o$.

5.1.2 Heterogeneous Synthetic Case A – Results

Using the models and well constrains defined on Section 3.1.2, we run two simulations until the maximum production was reached. The pseudo-steady state PI of each well was calculated following the workflow presented in Figure 3-4a on Section 3.2.1. Figure 5-2 shows the cumulative production over time, for each well, and their N_p ratio (gray dashed line). The continuous line represents the N_p values until a minimum flow rate of 20 m^3/d is reached. Table 5-1 summarizes the results obtained.

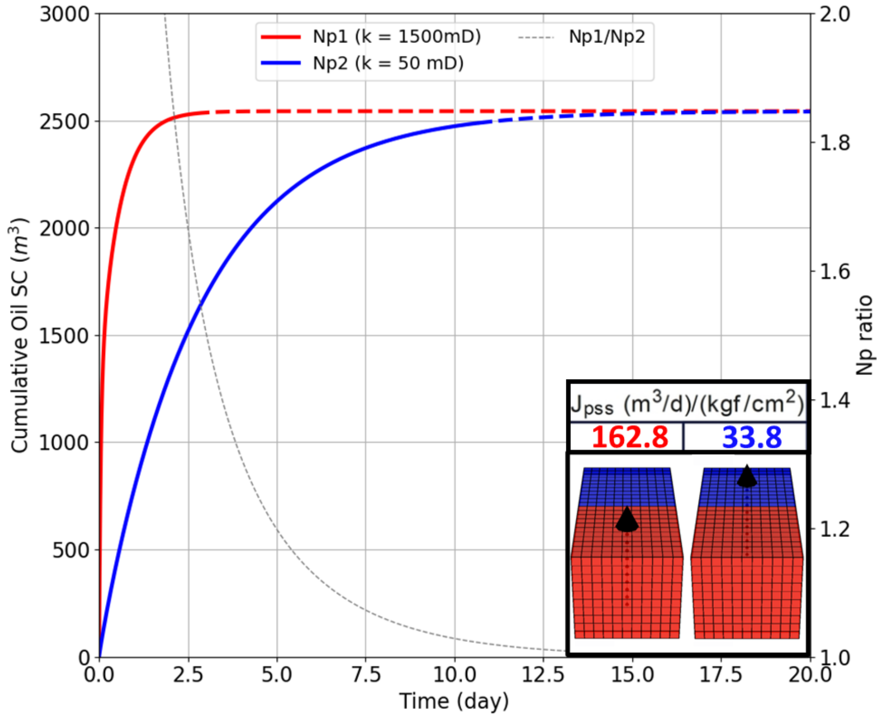

Figure 5-2: Synthetic model cumulative productions and its ratio for a single well on the 50 mD block and on the 1500 mD block.

Table 5-1: Synthetic model calculated properties

	PI (m³/d)/(kgf/cm²)		*N_{p1}/N_{p2}	N_{pmax} (m³)
	N_{p1}	N_{p2}		
$\Delta P = 27$ kgf/cm²	163	34	1.02	2543

**Values obtained at q = 20m³/d*

The slope of the cumulative production curves is proportional to the J_{pss} and its maximum value is independent. These results are in accordance with the limits presented for the analytical model by EQ8 and EQ9. Also, it is important to note that the Np ratio falls below 5% despite the productivity index ratio being approximately 5 times. This behavior is the same observed by the analytical model sensibility analysis presented in Figure 5-1. It is worth noting that the productivity index is directly correlated with oil anticipation, which affects the final NPV of the project.

5.1.3 Heterogeneous Synthetic Case B – Results

Using the models and well constraints defined on Section 3.1.3, we did two simulations until the maximum production was reached. The pseudo-steady state PI of each well was calculated following the workflow presented in Figure 3-4a on Section 3.2.1 and the values obtained, 163 $(m^3/d)/(kgf/cm^2)$ for N_{p1} and 33 $(m^3/d)/(kgf/cm^2)$ for N_{p2}, were similar to Case A, as expected. The differences can be attributed to numerical errors. Figure 5-3 shows the cumulative production of Case A (continuous) and case B (dashed) for each well.

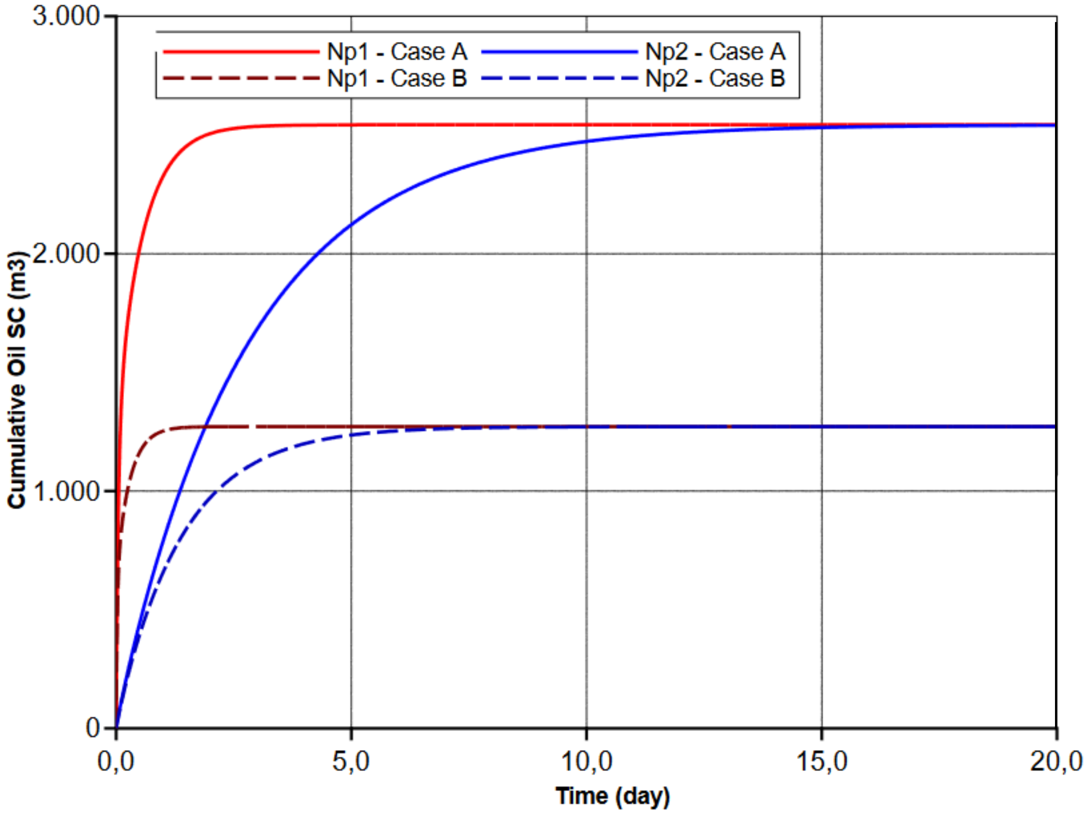

Figure 5-3: Cumulative production comparison between synthetic model case A and case B.

These results show the independence of the initial slope and the dependence of the maximum cumulative production with the total oil volume for a heterogeneous model. Those results are in accordance with the homogeneous analytical model obtained on Section 3.1.1, because the maximum N_p for Case B is exactly half the value of Case A (1272 m^3), as is the porosity. Also, the pseudo-steady state productivity index for Case B is equal Case A, making it independent of the porosity.

5.1.4 Heterogeneous Synthetic Case C - Results

Using the models and well constrains defined on Section 3.1.4, we did two simulations until the maximum production was reached. The pseudo-steady state PI of each well was calculated following the workflow presented on Figure 3-4a on Section 3.2.1 and the values obtained, 162 $(m^3/d)/(kgf/cm^2)$ for N_{p1} and 33.0 $(m^3/d)/(kgf/cm^2)$ for N_{p2}, were similar to Case A and Case B, as expected. The differences can be attributed to numerical errors. Figure 5-4 shows the cumulative production of Case A (continuous) and of Case C (dashed) for each well.

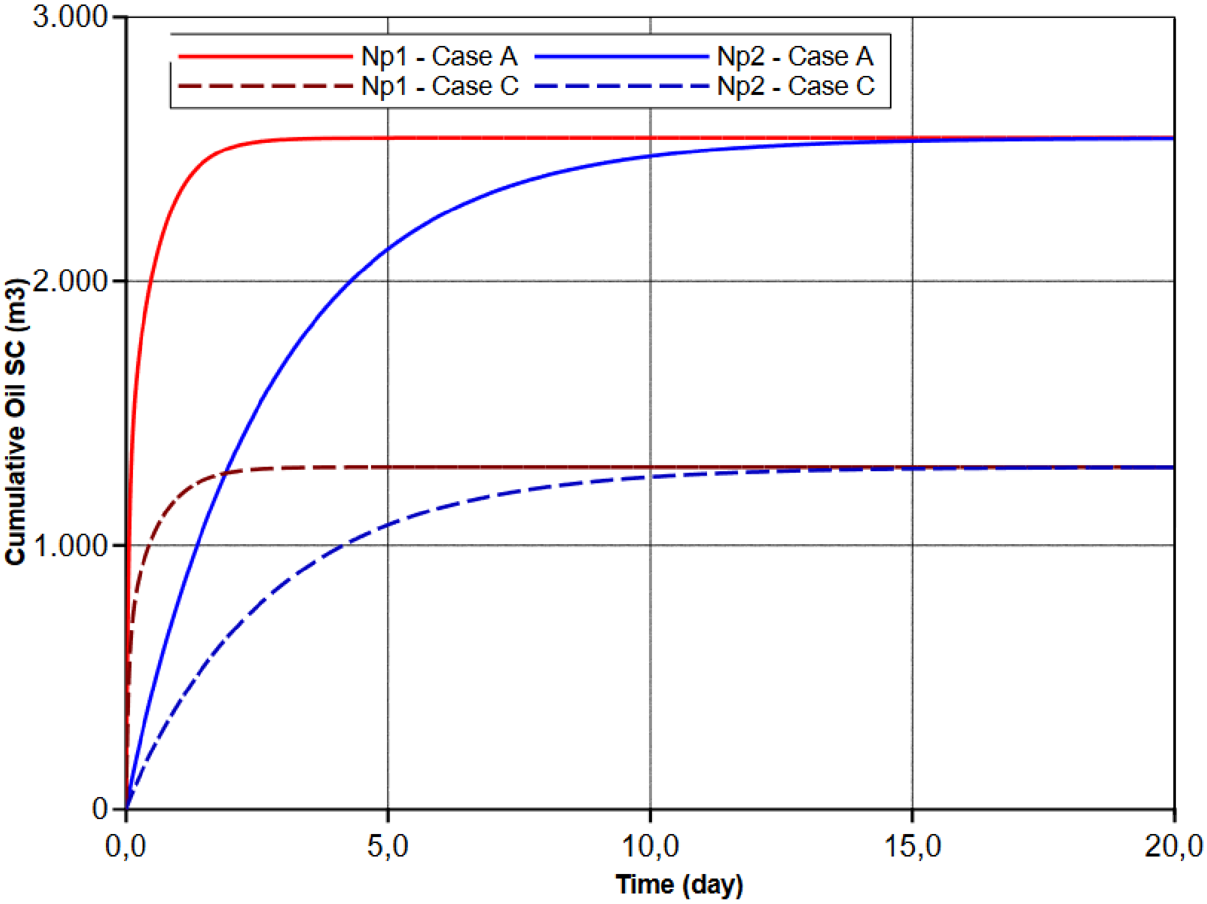

Figure 5-4: Cumulative production comparison between synthetic model case A and case C.

It can be noted that the maximum Np values obtained for Case C (1296 m^3) are very similar to those obtained for Case B (1272 m^3). This result is in accordance with the homogeneous analytical case, where a reduction in oil volume should have a similar response to a reduction in the pressure difference.

5.2 Namorado Field Benchmark Case

The quality map methods from Section 3.2.1 and Section 3.2.2 are applied to a real benchmark case based on Namorado Field in two scenarios, as discussed on Section 4.2. We start with the reference methodology, which is the cumulative production map, and compare its results with this work proposal, i. e., the productivity index map. Two different well constraints were used to build the PI map, constant bottom hole pressure and constant flow rate.

5.2.1 Cumulative Production Quality Map at Constant Bottom Hole Pressure

We first start with the reference method, which is the cumulative production map originally proposed by Cruz and Horne (1999), following the constraints and workflow presented on Section 3.2.2. Figure 5-5 contains the quality maps generated for both scenarios shown on Section 4.2, one considering the reservoir at its original pressure and the other considering the high block depleted due to a production history.

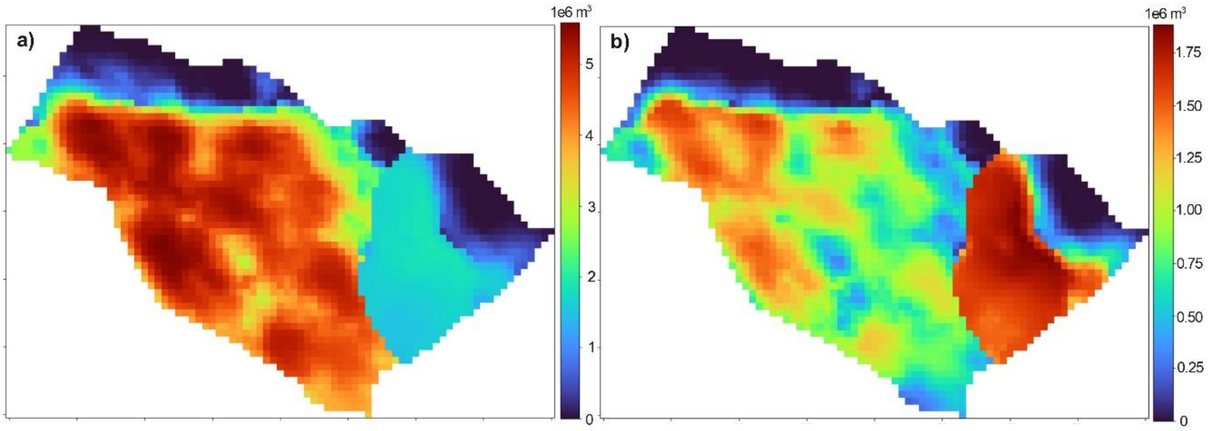

Figure 5-5: Cumulative production quality maps for (a) high block initially at the original pressure; (b) high block initially depleted

Both maps have distinct color scale ranges, and even so, there is a difference between them. When the entire reservoir is initially at its original pressure (Figure 5-5a), the quality index values based on the cumulative production for the high block are higher than those calculated for the low block. Otherwise, in the initially depleted case (Figure 5-5b), the low block showed a higher anomaly. Does that mean the low block has a better production potential than the high block after the production period? The answer is no. From EQ11, we can see that the primary production is dependent on the product of oil volume ($N.B_{oi}$) by the pressure difference (p_{avg}-p_{wf}). In both scenarios, (a) and (b), the relation between the remaining oil volumes is nearly the same, around 3 times, as shown in Table 5-2. Also, since the same value for bottom-hole pressure was set on both cases and blocks, the pressure difference of the high block has reduced around 10 times from scenario (a) to scenario (b) due to primary depletion. This caused the product between the oil volume and the pressure difference changes from 19376 MM $m^3.kgf/cm^2$ to 2076 MM $m^3.kgf/cm^2$ for the high block, as stated in Table 5-2. The low block product value of 5745 MM $m^3.kgf/cm^2$ did not change, becoming higher than the high block in scenario (b), causing the inversion of the anomalies.

Table 5-2: Oil Volume times the Pressure Difference Blocks Comparison

	Case a)			Case b)		
Block	OIP (MM m3)	$(p_{avg}-p_{wf})$ kgf/cm^2	$N.B_{oi}.(p_{avg}-p_{wf})$	OIP (MM m^3)	$(p_{avg}-p_{wf})$ kgf/cm^2	$N.B_{oi}.(p_{avg}-p_{wf})$
High Block	138.4	140	19376	134.3	15	2076
Low Block	41.1	140	5745	41.1	140	5745

5.2.2 Productivity Index Quality Map at Constant Flow Rate

The productivity index quality map, which is the proposal of this research, was built following the workflow of Figure 3-4a on Section 3.2.1. We used the same scenarios for the reference method. Figure 5-6 contains the maps generated at a constant flow rate of 10 m^3/d. A small flow rate was chosen to keep the bottom-hole pressures above the bubble point (P_b = 210 kgf/cm^2).

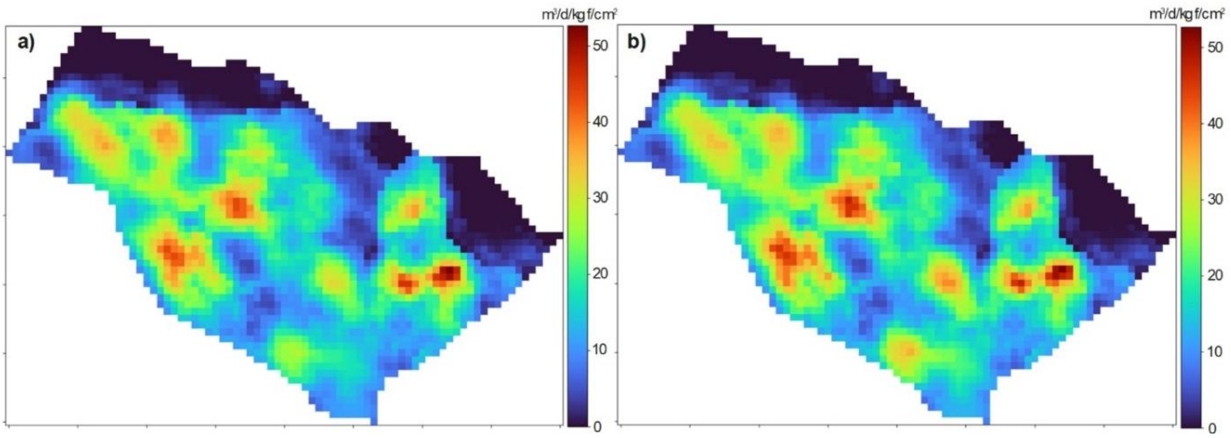

Figure 5-6: Productivity index maps for (a) high block initially at the original reservoir pressure; (b) high block initially depleted

It is important to point out that both maps have the same color scale. Anomalies of the low block can now be seen and the quality map has similar responses on both scenarios. That occurs because the oil fluid properties variation is small for undersaturated reservoirs, and the produced volume in scenario b) is not enough to cause a relative permeability change due to a water saturation change. The productivity index map is invariant to the reservoir mean pressure and is directly correlated with the production potential. Its value is also independent of the product $N.B_{oi}.\Delta p.c_{eo}/B_o$, making it a good parameter to compare the production potential of different hydraulic disconnected regions of the reservoirs. Different from the Np values, productivity index is a property measured in the field, making this map comparable with field tests.

5.2.3 Productivity Index Quality Map at Constant Bottom Hole Pressure

The productivity index quality map at constant bottom hole pressure was built following the same workflow for the constant flow rate, shown in Figure 3-4 on Section 3.2.1. Three different constant BHP were used to generate the maps, these being.250 kgf/cm^2 (Figure 5-7), 190 kgf/cm^2 (Figure 5-8) and 100 kgf/cm^2 (Figure 5-9). The bubble point pressure is 210 kgf/cm^2, so the first map is well above that pressure, the second is just below and is the BHP suggested by the optimization study case, and the last one is well below it. They were generated only for the scenario of the high block at its original pressure, with regions close to the aquifer being neglected to speed up the process.

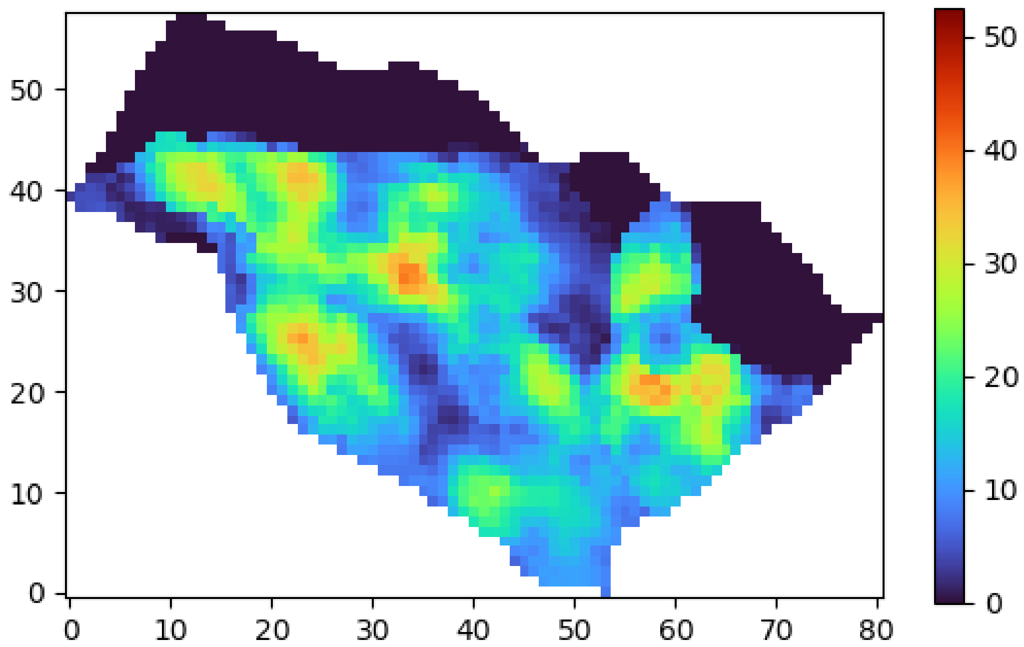

Figure 5-7: Productivity index map at a constant bottom hole pressure of 250kgf/cm^2 (P_b = 210 kgf/cm^2)

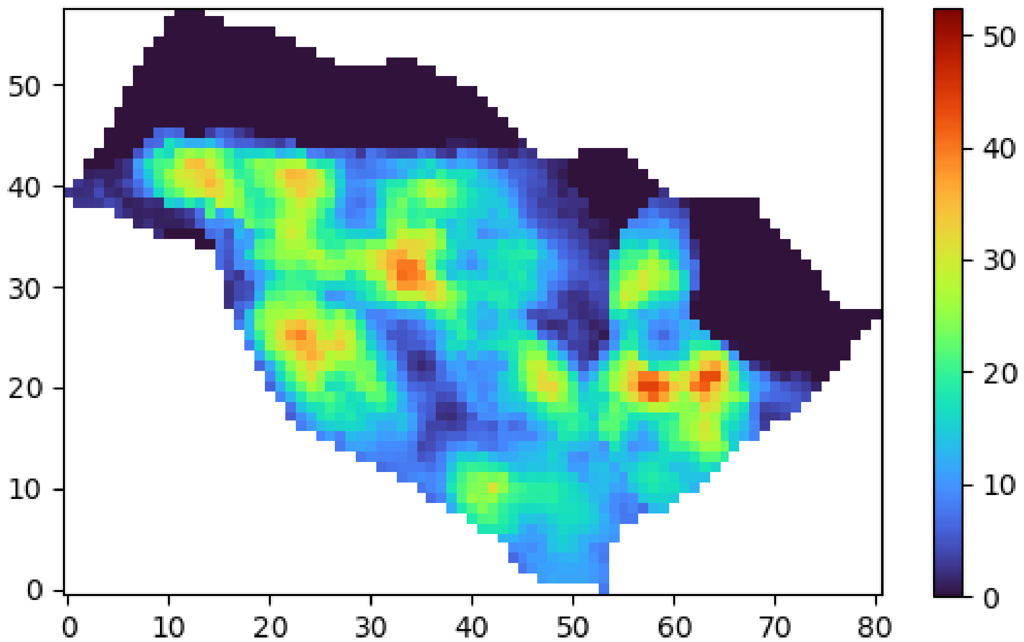

Figure 5-8: Productivity index map at a constant bottom hole pressure of 190kgf/cm² (P_b = 210 kgf/cm²)

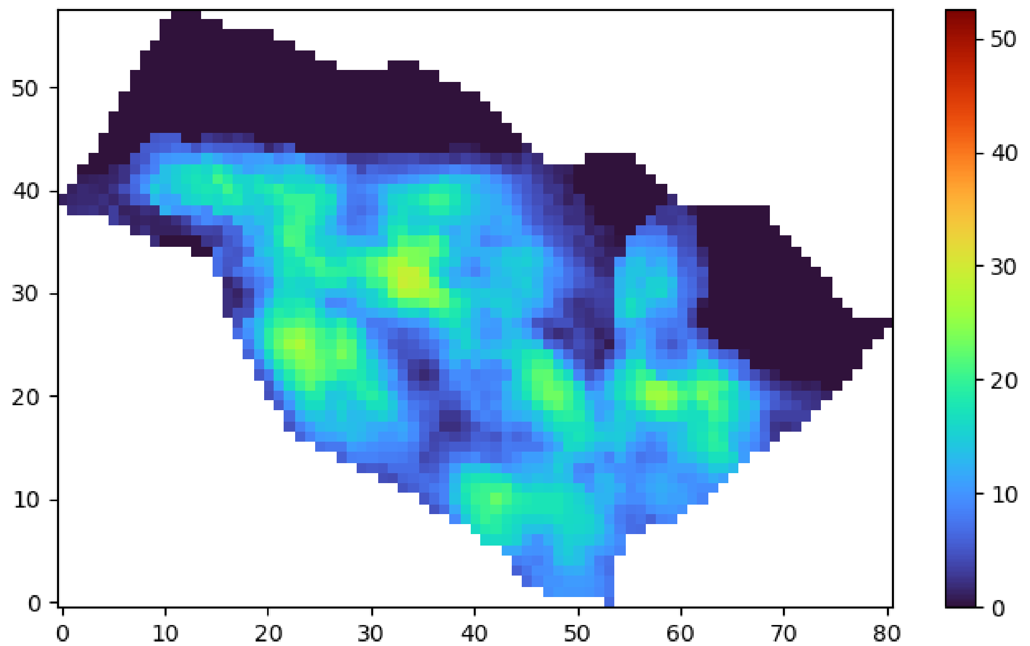

Figure 5-9: Productivity index map at a constant bottom hole pressure of 100kgf/cm² (P_b = 210 kgf/cm²)

Analyzing the three maps presented here, which have the same color scale,and comparing them with the constant flow rate maps obtained on Section 5.2.2, we can see the same positions of the anomalies. These results are expected since constant flow rate and constant bottom hole pressure shape factors have similar values (Section 2.1). It can be noted similar PI values for the BHP maps of 250 kgf/cm^2 and 190 kgf/cm^2, while the map with 100 kgf/cm^2 has lower values. This happens because the gas, released from the oleic phase, when the reservoir average pressure falls below the bubble pressure, lowers the oil production potential, as can be seen on Vogel (1968) empirical model.

5.2.4 Comparison of Applied Methods

To do a practical and quantitative comparison between the cumulative production map and the productivity index map, we made a crossplot between each map and each scenario. Figure 5-10 presents this plot for the high block at its original and depleted pressure (D.P.), and the low block at its original pressure (O.P.). The low block depleted was not plotted twice, because it wasn't affected by the production history of the high block.

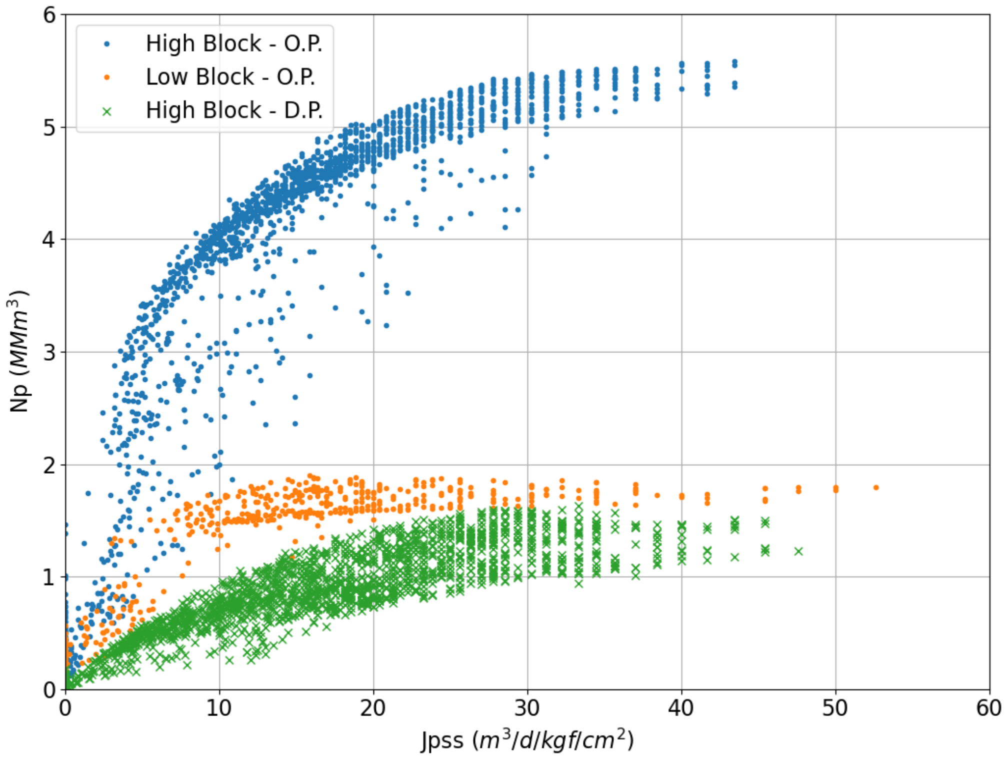

Figure 5-10: Crossplot between productivity index and cumulative production map.

It is noticeable that we can have the same value of productivity index for different values of cumulative production. These results are in accordance with the analytical model sensibility analysis (Figure 5-1) and the synthetic studies presented on Section 4.1.1.

5.3 Productivity Index Map Validation Results

The methods used for the qualitative and quantitative validation are described on Section 3.3. Here the results are presented and compared with the constant flow rate productivity index map.

5.3.1 Qualitative Analysis

A qualitative analysis of the productivity index map was made comparing its anomalies with the vertical well positions of the obtained optimized strategy, detailed on Appendix B, following the methodology presented on Section 3.3.1. Figure 5-11 shows the productivity index map with the final optimized well positions. Table 5-3 compares the cumulative oil and water production, net present value and recover factor of the obtained strategy with other ones presented in the literature.

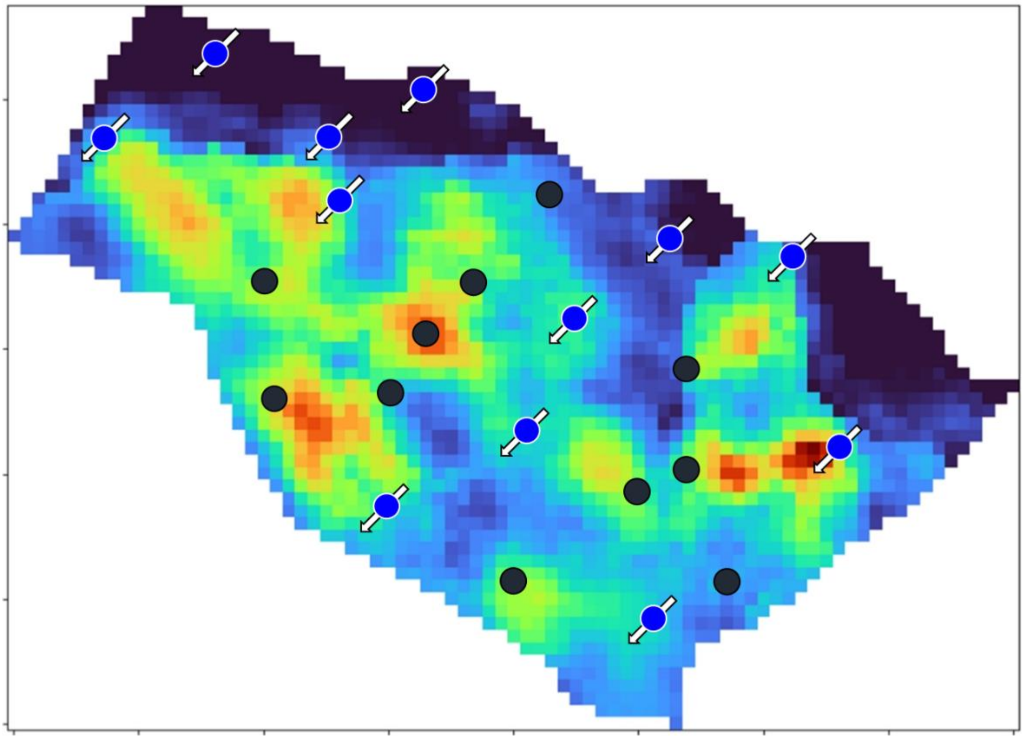

Figure 5-11: Well positions of the vertical well optimized strategy over the productivity index map

The strategy obtained is in accordance with others reported in the literature (Gaspar *et al.*, 2016; De Moraes; Coelho, 2022; Santos *et al.*, 2021; Plukmonton, 2017). From Table 5-3, it is noticeable that the high block and low block have similar recovery factors, reinforcing the example shown in Figure 5-5 on Section 5.2.1.

Table 5-3: Vertical Well Optimized Strategy Comparison

Work	Region / Strategy	Nº Wells	Np (MM m3)	Wp (MM m3)	NPV (Bi USD)	RF (%)
Developed by the author	High Block	18	56.5	40.1	-	56.4
	Low Block	5	16.4	8.4	-	53.8
	Total	23	72.6	48.5	2.72	55.8
(Gaspar *et al.*, 2016)	Total / Str. A	22	-	-	2.47	56.2
(Plukmonton, 2017)	Total	-	51.2	46.7	-	-
(Santos *et al.*, 2021)	Total	-	-	-	2.51	-
(De Moraes; Coelho, 2022)	Total / MOEA D-NFTS	20	70.0	45.2	-	-

Figure 5-11 also shows the good correlation between the producers positions and the productivity index anomalies. They are not necessarily located on the highest values because of the following factors: 1) wells have an upper flow rate limit, which means there is no difference in production above a certain PI value; 2) The distance between producers and injectors is an important optimization factor. Short distances may have early water production while long distances may delay the field pressure maintenance to a higher production rate; 3) Each well has a maximum oil recoverable volume within the project timeline, meaning that a well positioned in the area correspondent to a lower PI justifies the increase on the total project oil recovery factor.

5.3.2 Quantitative Analysis

Using the producers positions of the strategy presented on Figure 4-11, we opened all of them at the same time, while keeping the injectors closed. The individual well productivity index contribution for the multi-well system scenario was obtained using the methodology presented in Figure 3-7a and Section 3.3.2, i.e., using the multi-well model proposed by Marhaendrajana and Blasingame (2001). These values were compared with those obtained from the productivity index map of Figure 4-6a, which represents an individual well PI on a single well system i.e. without interference from other wells.

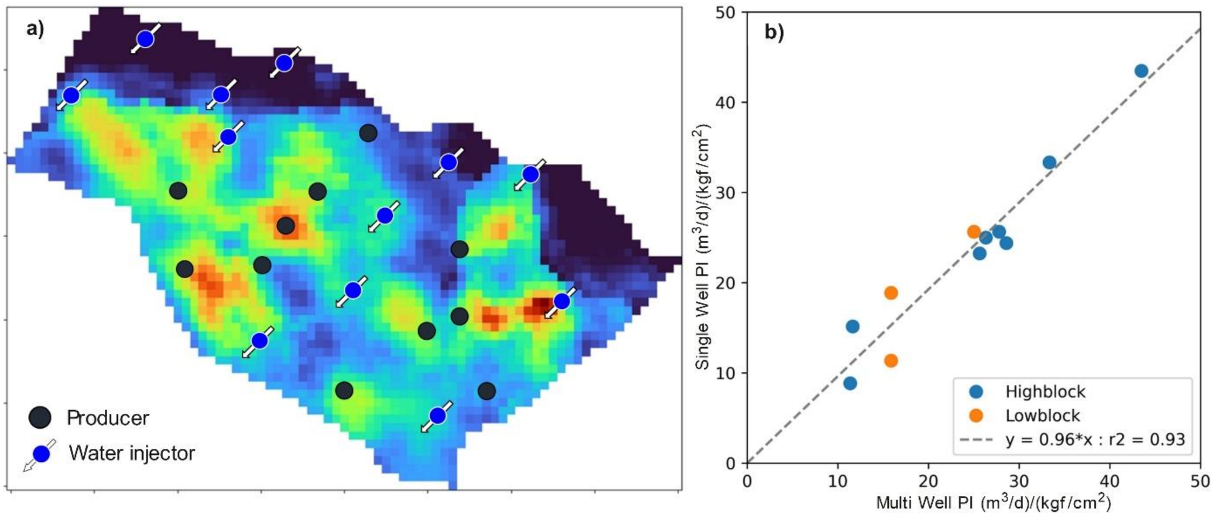

Figure 5-12: (a) optimized position of 11 vertical producers and 12 vertical injectors with the productivity index map as background; (b) single well x multi well Jpss correlation.

The results show a good correlation between the single well system Jpss and multi-well system Jpss, with R2 = 0.93. Also, the slope is close to one, which is reasonable because the Jpss varies with the inverse of the natural logarithm of the drainage volume. Using EQ18 we made a sensitivity analysis of the productivity index ratio with the drainage area. Figure 5-13 and Figure 5-14 shows the PI ratio (J_{pss1}/J_{pss2}) for increasing A_1 drainage areas on x-axis and decreasing A_2 drainage areas related to A_1 on y-axis where $A_2 = A_1/\alpha$. Two different constant flow rate shape factors were used, related to a well in the center and a well on the corner, respectively.

Drainage Area A_1 (m^2)

α parameter

	1.00E+03	1.00E+04	1.00E+05	1.00E+06	1.00E+07	1.00E+08
1	1.00	1.00	1.00	1.00	1.00	1.00
2	0.92	0.94	0.95	0.96	0.96	0.97
3	0.87	0.90	0.92	0.93	0.94	0.95
4	0.84	0.87	0.90	0.91	0.92	0.93
5	0.82	0.85	0.88	0.90	0.91	0.92
6	0.79	0.84	0.87	0.89	0.90	0.91
7	0.78	0.82	0.85	0.88	0.89	0.90
8	0.76	0.81	0.84	0.87	0.88	0.90
9	0.75	0.80	0.84	0.86	0.88	0.89
10	0.74	0.79	0.83	0.85	0.87	0.89
11	0.72	0.78	0.82	0.85	0.87	0.88
12	0.71	0.77	0.81	0.84	0.86	0.88

$C_A = 31.6$ *(centered well)*

Figure 5-13: Pseudo Steady State PI variation with drainage area for a centralized well (C_A = 31.6)

α parameter

	1.00E+03	1.00E+04	1.00E+05	1.00E+06	1.00E+07	1.00E+08
1	1.00	1.00	1.00	1.00	1.00	1.00
2	0.95	0.96	0.96	0.97	0.97	0.97
3	0.92	0.93	0.94	0.95	0.95	0.96
4	0.90	0.92	0.93	0.94	0.94	0.95
5	0.89	0.90	0.92	0.92	0.93	0.94
6	0.88	0.89	0.91	0.92	0.92	0.93
7	0.87	0.88	0.90	0.91	0.92	0.93
8	0.86	0.88	0.89	0.90	0.91	0.92
9	0.85	0.87	0.88	0.90	0.91	0.92
10	0.84	0.86	0.88	0.89	0.90	0.91
11	0.83	0.86	0.87	0.89	0.90	0.91
12	0.83	0.85	0.87	0.88	0.90	0.90

$C_A = 0.1$ *(corner well)*

Figure 5-14: Pseudo Steady State PI variation with drainage area for a corner well (C_A = 0.1)

The results above show that independent of the well position, the J_{pss} ratio doesn’t vary significantly, even if we decrease the drainage area for a factor higher than 10 ($\alpha > 10$). This means that it is not expected a big difference between the productivity index obtained by a single well and a multi-well system due to the size of the drainage area size.

6 CONCLUSIONS AND FUTURE WORK

6.1 Conclusions

The work presented here was mainly motivated by the need of generating a quality map that directly correlate with well production potential, allowing the comparison of non-communicated areas inside a specific reservoir or different reservoirs. This comparative tool would assist on positioning producer wells to define an initial production strategy or on optimizing the wells position by delimitating the search space at the sweet spots, and therefore reducing the strategy optimization computational cost.

Aiming to achieve that, the main focus was to generate a quality map based on the productivity index and compare its results with the quality map based on cumulative production, which is one of the most applied methods nowadays. First, it was presented the proper definition of the productivity index, i.e., the ratio of the flow rate by the difference between the average reservoir pressure and the wellbore pressure. This property represents the oil mobility and is measured on the field during the life cycle of a reservoir through pressure transient analysis and production tests, and it can be quantitatively correlated with the proposed quality map.

Through analytical and synthetic models presented here, we were able to highlight the importance of the productivity index and its role on the cumulative production. Summarily, PI is directly proportional to the production anticipation and its anomalies are independent of the reservoir initial pressure and well bottom hole producing pressure or instantaneous flow rate. The real case application showed its anomaly positions invariance when dealing with disconnected regions or depleted reservoirs, considering initial reservoir pressure conditions above or below the bubble pressure. Also, its value on a multi-well system is close to its value on a single well system, making the results obtained by the map reliable when taking well interference into account. In addition, using the multi well scenario, the time for the PI map generation can be reduced.

Productivity index represents the effective mobility of the fluid being displaced. Then, on a scenario with gas flow or water production, PI is proportional to the oil relative mobility on that specific reservoir condition. That was showed even when the production pressure was below the bubble point, demonstrated the application of the presented methodology on depleted saturated reservoirs. The constant bottom hole pressure or flow rate assumption is not also a limitation, as the productivity index is same with a variable bottom hole pressure production or a variable flow rate.

All those characteristics confers many advantages to the application of the productivity index as the parameter used to build quality maps. Those advantages were demonstrated starting from a simplified analytical model to a real field application allowing the following conclusions and observations of the following points:

1) Productivity index is constant under pseudo-steady state, making it a good parameter to represent the production potential of a reservoir.

2) The sweet spots for the productivity index map are invariant over pressure difference and total oil volume, allowing to compare the production potential between isolated reservoir regions or different reservoirs.

3) The correlation between the single-well and multi-well productivity index was higher than 90%, i. e, R2=0.93, making the quality map based on the productivity index a suitable tool to assist in a production development strategy.

4) Productivity index represents the displaced fluid mobility and can be obtained through field tests allowing comparative analyses among the quality map sweet spots and the wellbores measured data.

5) Productivity index maps can be applied to saturated and depleted reservoirs

6.2 Future Work

This work was done considering vertical wells and pseudo-steady state flow regime. The productivity index theory is well stablished for vertical, horizontal wells and fracture reservoirs (Guo et al. 2008), and the method proposed in this work could be applied considering those conditions. The same consideration is valid for unconventional reservoirs, where longer simulation times can allow reaching the pseudo-steady state. Also, an injectivity index map could be generated in the same way to identify the well injectors sweet spots. If coupled with the productivity index map, an initial ratio of producers/injectors could be estimated. Finally, the productivity index quality map could be faster built by using the multi-well analytical model and spatial interpolation.

REFERENCES

AHMED. **Advanced Reservoir Engineering**., 2005.

ARPS, J. J. Analysis of Decline Curves. **Transactions of the AIME**, vol. 160, no. 01, p. 228–247, 1 Dec. 1945. https://doi.org/10.2118/945228-G.

AVANSI, G. D.; SCHIOZER, D. J. UNISIM-I: Synthetic Model for Reservoir Development and Management Applications. **International Journal Of Modeling and Simulation for the Petroleum Industry**, vol. 9, no. 1, 2015. .

BABU, D. K.; ODEH, A. S. Productivity of a Horizontal Well. **SPE Reservoir Engineering**, 1989. .

CAVALCANTE FILHO, J. S. de A. Methodology for Quality Map Generation to Assist with the Selection and Refinement of Production Strategies. *In*: SPE ANNUAL TECHNICAL CONFERENCE AND EXHIBITION, 9 Oct. 2005. **All Days** [...]. Dallas, Texas: SPE, 9 Oct. 2005. p. SPE-101940-STU. DOI 10.2118/101940-STU. Available at: https://onepetro.org/SPEATCE/proceedings/05ATCE/All-05ATCE/SPE-101940-STU/72364. Accessed on: 19 Jul. 2023.

COMPAM, A. L. M. Ensaios de Permeabilidade Relativa e Pressão Capilar Gás-Óleo de Amostras de Poço. **CT-TRA 030/09**, 2009. .

COTTINI-LOUREIRO, A.; ARAUJO, M. Optimized Well Location by Combination of Multiple Realization Approach and Quality Map Methods. 2005. .

CRUZ, P. S. da; HORNE, R. The Quality Map: A Tool for Reservoir Uncertainty Quantification and Decision Making. Oct. 1999. https://doi.org/10.2118/56578-MS.

CULLICK, A. S.; NARAYANAN, K.; GORELL, S.; DIGITAL, H.; SOLUTIONS, C. Optimal Field Development Planning of Well Locations With Reservoir Uncertainty. 2005. https://doi.org/10.2118/96986-MS.

DE MORAES, M. B.; COELHO, G. P. A diversity preservation method for expensive multi-objective combinatorial optimization problems using Novel-First Tabu Search and MOEA/D. **Expert Systems with Applications**, vol. 202, p. 117251, Sep. 2022. https://doi.org/10.1016/j.eswa.2022.117251.

DIETZ, D. N. Determination of Average Reservoir Pressure From Build-Up Surveys. **Journal of Petroleum Technology**, vol. 17, no. 08, p. 955–959, 1 Aug. 1965. https://doi.org/10.2118/1156-PA.

DIYASHEV, I. R.; ECONOMIDES, M. J. The Dimensionless Productivity Index as a General Approach to Well Evaluation. **SPE Production & Operations**, vol. 21, no. 03, p. 394–401, 19 Aug. 2006. https://doi.org/10.2118/94644-PA.

DOUBLET, L. E.; PANDE, P. K.; MCCOLLUM, T. J. Decline Curve Analysis Using Type Curves - Analysis of Oil Well Production Data Using Material Balance Time: Application to Field Cases. **Society of Petroleum Engineers**, 1994. .

FETKOVICH, M. J. Decline Curve Analysis Using Type Curves. **JOURNAL OF PETROLEUM TECHNOLOGY**, 1980. .

GASPAR, A. T. F. S.; BARRETO, C. E. A. G.; SCHIOZER, D. J. Assisted process for design optimization of oil exploitation strategy. **Journal of Petroleum Science and Engineering**, vol. 146, p. 473–488, Oct. 2016. https://doi.org/10.1016/j.petrol.2016.05.042.

GASPAR, A. T.; SANTOS, A.; MASCHIO, C.; AVANSI, G.; HOHENDORFF, J. .; SCHIOZER, D. J. UNISIM-I-D. Dec. 2023. Available at: https://www.unisim.cepetro.unicamp.br/benchmarks/br/unisim-i/unisim-i-d. Accessed on: 27 Dec. 2023.

GASPAR, A. T.; SANTOS, A.; SCHIOZER, D.; FILHO, J. H. Case Study for Field Development and Management - Selection of Production Strategy based on UNISIM-II. 2023. .

GUO, B.; SUN, K.; GHALAMBOR, A. **Well productivity handbook: vertical, fractured, horizontal, multilateral, and intelligent wells**. Houston, TX: Gulf Pub, 2008.

GUTHRIE, R. K.; GREENBERGER, M. H. The use of multiple-correlation analyses for interpreting petroleum-engineering data. **Drilling and Production Practice**, , p. 130–137, 1955. .

HAIDER, M. L. The Productivity Index. **Transactions of the AIME**, vol. 123, no. 01, p. 112–119, 1 Dec. 1937. https://doi.org/10.2118/937112-G.

HELMY. New Shape Factors for Wells Produced at Constant Pressure. 1998. .

LE RAVALEC, M. Optimizing Well Placement With Quality Maps Derived From Multi-fidelity Meta-models. *In*: SPE EUROPEC/EAGE ANNUAL CONFERENCE, 4 Jun. 2012. **All Days** [...]. Copenhagen, Denmark: SPE, 4 Jun. 2012. p. SPE-154416-MS. DOI 10.2118/154416-MS. Available at: https://onepetro.org/SPEEURO/proceedings/12EURO/All-12EURO/Copenhagen,%20Denmark/157226. Accessed on: 12 Sep. 2023.

LEE, J.; ROLLINS, J. B.; SPIVEY, J. P. **Pressure Transient Testing**. [*S. l.*]: Society of Petroleum Engineers, 2003. DOI 10.2118/9781555630997. Available at: https://onepetro.org/books/book/21/Pressure-Transient-Testing. Accessed on: 28 Jul. 2023.

MARHAENDRAJANA, T.; BLASINGAME, T. A. Decline Curve Analysis Using Type Curves - Evaluation of Well Performance Behavior in a Multiwell Reservoir System. 2001. https://doi.org/10.2118/71517-MS.

MASCHIO, C.; NAKAJIMA, L.; SCHIOZER, D. J. Production Strategy Optimization Using Genetic Algorithm and Quality Map. *In*: EUROPEC/EAGE CONFERENCE AND EXHIBITION, 9 Jun. 2008. **All Days** [...]. Rome, Italy: SPE, 9 Jun. 2008. p. SPE-113483-

MS. DOI 10.2118/113483-MS. Available at: https://onepetro.org/SPEEURO/proceedings/08EURO/All-08EURO/SPE-113483-MS/144123. Accessed on: 23 Aug. 2023.

MIRZAEI-PAIAMAN, A.; GHANBARIAN, B. A new method for characterizing dynamic reservoir quality: Implications for quality maps in reservoir simulation and rock type classification. **Journal of Petroleum Science and Engineering**, vol. 218, p. 111049, Nov. 2022. https://doi.org/10.1016/j.petrol.2022.111049.

MOORE, T. V. 1930. .

MUSKAT. **The Flow of Homogeneous Fluids Through Porous Media**. [*S. l.*: *s. n.*], 1946.

NAKAJIMA, L.; SCHIOZER, D. J. Horizontal Well Placement Optimization Using Quality Map Definition. *In*: CANADIAN INTERNATIONAL PETROLEUM CONFERENCE, 2003. **Canadian International Petroleum Conference** [...]. Calgary, Alberta: Petroleum Society of Canada, 2003. DOI 10.2118/2003-053. Available at: http://www.onepetro.org/doi/10.2118/2003-053. Accessed on: 20 Jul. 2023.

NASRABADI, H.; MORALES, A.; ZHU, D. Well placement optimization: A survey with special focus on application for gas/gas-condensate reservoirs. **Journal of Natural Gas Science and Engineering**, vol. 5, p. 6–16, Mar. 2012. https://doi.org/10.1016/j.jngse.2011.10.002.

PLUKMONTON, P. **APPLICATION OF ENSEMBLE-BASED OPTIMIZATION**. 2017. Tese – Texas A&M University, 2017.

RAVAGNANI, A. T. F. da S. G.; MAZO, E. O. M.; SCHIOZER, D. J. A CASE STUDY OF THE STRUCTURE OF THE PROCESS FOR PRODUCTION STRATEGY SELECTION. **Int. J. Model. Simul. Pet. Ind.**, , p. 4–5, 9–15, 2011. .

RODRIGUEZ, F.; CINCO-LEY, H. A New Model for Production Decline. 1993. .

SANTOS, S. M. G.; GASPAR, A. T. F. S.; SCHIOZER, D. J. Information, robustness, and flexibility to manage uncertainties in petroleum field development. **Journal of Petroleum Science and Engineering**, vol. 196, p. 107562, Jan. 2021. https://doi.org/10.1016/j.petrol.2020.107562.

VAN EVERDINGEN, A. F.; HURST, W. The Application of the Laplace Transformation to Flow Problems in Reservoirs. **Journal of Petroleum Technology**, vol. 1, no. 12, p. 305–324, 1 Dec. 1949. https://doi.org/10.2118/949305-G.

VOGEL, J. V. Inflow Performance Relationships for Solution-Gas Drive Wells. **Journal of Petroleum Technology**, vol. 20, no. 01, p. 83–92, 1 Jan. 1968. https://doi.org/10.2118/1476-PA.

VOGUEL IPR. 2024. **pengtools**. Available at: https://wiki.pengtools.com/images/c/cd/Constant_PI_and_Vogel%27s_IPR.png. Accessed on: 12 Jun. 2024.

WARSZAWSKI, A.; FERREIRA, C. A. S. Comparison between well test results of vertical and horizontal well on Quissamã Formation, Campos Basin. *In*: 13TH INTERNATIONAL CONGRESS OF THE BRAZILIAN GEOPHYSICAL SOCIETY & EXPOGEF, RIO DE JANEIRO, BRAZIL, 26-29 AUGUST 2013, 29 Aug. 2013. **13th International Congress of the Brazilian Geophysical Society & EXPOGEF, Rio de Janeiro, Brazil, 26–29 August 2013** [...]. Rio de Janeiro, Brazil: Brazilian Geophysical Society, 29 Aug. 2013. p. 4–10. DOI 10.1190/sbgf2013-002. Available at: https://library.seg.org/doi/10.1190/sbgf2013-002. Accessed on: 27 Dec. 2023.

WARSZAWSKI, A.; FERREIRA, C. A. S. Well test analysis integrated with the geologic context of the Macaé Formation in Campos Basin, Brazil. *In*: 12TH INTERNATIONAL CONGRESS OF THE BRAZILIAN GEOPHYSICAL SOCIETY & EXPOGEF, RIO DE JANEIRO, BRAZIL, 15-18 AUGUST 2011, 18 Aug. 2011. **12th International Congress of the Brazilian Geophysical Society & EXPOGEF, Rio de Janeiro, Brazil, 15–18 August 2011** [...]. Rio de Janeiro, Brazil: Brazilian Geophysical Society, 18 Aug. 2011. p. 84–89. DOI 10.1190/sbgf2011-019. Available at: https://library.seg.org/doi/10.1190/sbgf2011-019. Accessed on: 27 Dec. 2023.

WEIMER, P. (Ed.). **Producibility of Turbidite Reservoirs - A Comparison of the North Sea and Gulf of Mexico**. [*S. l.*]: SOCIETY OF ECONOMIC PALEONTOLOGISTS AND MINERALOGISTS, 2000. DOI 10.5724/gcs.00.20. Available at: http://gcsproceedings.sepmonline.org/content/gcssepmproc/gcs015/1.toccontent/20. Accessed on: 27 Dec. 2023.

WOOD, D. A.; CAI, J. Production decline curve analysis and reserves forecasting for conventional and unconventional gas reservoirs. **Sustainable Natural Gas Reservoir and Production Engineering**. [*S. l.*: *s. n.*], 2021.

APPENDIX A: Dimensionless Variables

$$J_{Dpss} = J_{pss}\frac{B_o\mu_o}{2\pi k_o h} \quad \text{(EQA1)}$$

$$t_{DA} = \frac{k_o t}{\phi\mu_o c_t A} \quad \text{(EQA2)}$$

$$q_D = \frac{Q_o\mu_o B_0}{2\pi k_o h\left(p_i - p_{wf}\right)} \quad \text{(EQA3)}$$

$$N_{Dp}(t_D) = \frac{N_p(t)B_0}{2\pi\phi c_t h r_w^2\left(p_i - p_{wf}\right)} \quad \text{(EQA4)}$$

APPENDIX B: Namorado Field Optimization Strategy Development

APPENDIX B1: History Match

A history match was done with the model UNISIM-I-D adjusting the oil and water relative permeabilities at the residual oil and irreducible water saturation. The final values obtained are in accordance for a sandstone model in the literature (Compam, 2009) and are presented on Table 7-1.

Table 7-1: History Match Parameters

	K_{ro} ($S_{wi=17\%}$)	K_{rw} ($S_{or=18\%}$)
Initial Model	0.41	0.58
Adjusted Model	0.65	0.22

The mean pressure and the field oil and water cumulative production data of the model are displayed on Figure 7-1: Field curves before (dashed) and after (continuous) history match for (a) mean reservoir pressure and (b) reservoir cumulative oil and water production. with the curves match before (dashed) and after the matching (continuous).

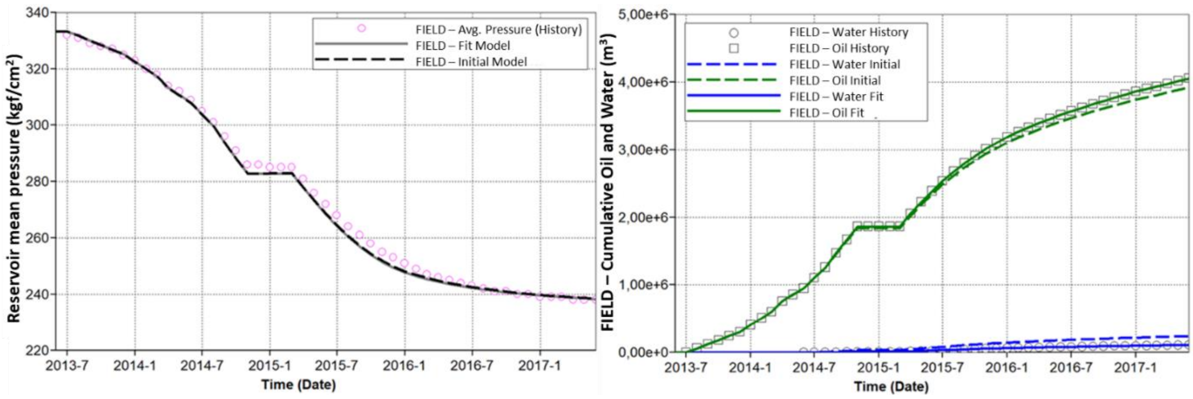

Figure 7-1: Field curves before (dashed) and after (continuous) history match for (a) mean reservoir pressure and (b) reservoir cumulative oil and water production.

The oil and water rate of two wells that were mismatched are shown on Figure 7-2: Main well flow rate before (dashed) and after (continuous) history match for (a) oil rate and (b) water rate.

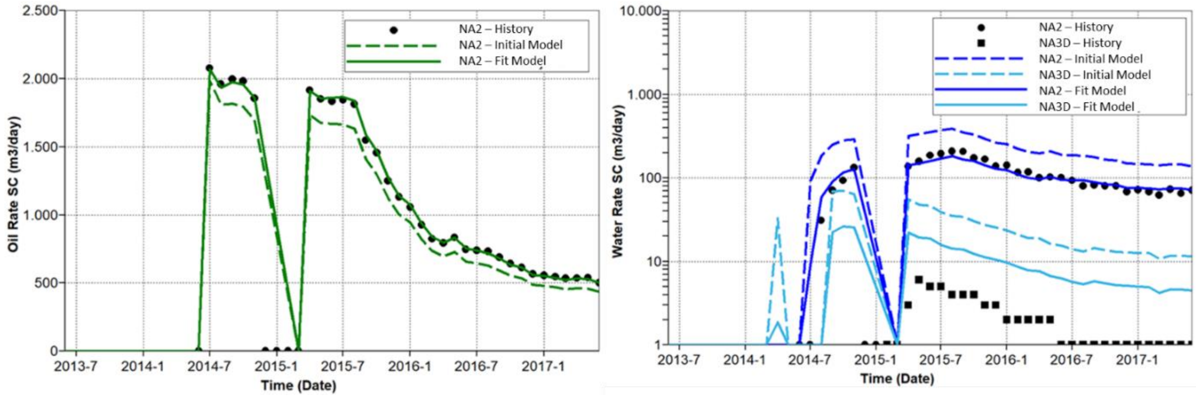

Figure 7-2: Main well flow rate before (dashed) and after (continuous) history match for (a) oil rate and (b) water rate.

APPENDIX B2: Initial Strategy Development

To define an initial strategy that will be later optimized the user needs to define a well type (injector or producer, vertical, horizontal or slanted), initial number of producers, injectors and its positions. On this particular case we assumed vertical wells. The number of producers was defined as the ratio between the recoverable oil and the potential cumulative production of a well, as showed on EQB1.

$$n_{prod} = \frac{VOIP * RF}{Np} \qquad \text{(EQB1)}$$

VOIP is given by the model, while the recovery factor and the cumulative potential production need to be estimated. Recovery factor was estimated using an empirical sandstone model proposed by Guthrie and Grennberger (1955), using static and dynamic reservoir properties as showed on EQB2.

$$RF = 0.27\,log(k) - 0.14\,log(\mu_o) - 1.54\phi\ - 0.00035h + 0.26Sw + 0.11 \qquad \text{(EQB2)}$$

Where RF is the recovery factor, μ_o the oil viscosity, ϕ the effective porosity, h is the netpay and S_w is the water saturation. Table 7-2: Mean Reservoir and Fluid Parameters of Namorado Field lists the mean values and standards deviations obtained for each parameter and the calculated recovery factor.

Table 7-2: Mean Reservoir and Fluid Parameters of Namorado Field

Log10(k) (mD)	h (m)	ϕ_e (dec)	μ_0 (cP)	Sw (Fraction)	RF (Fraction)
1.7 +- 0.7	72 +- 25	0.14 +- 0.08	0.84 +- 0.1	0.18 +- 0.04	0.4 +- 0.2

The cumulative production potential was obtained through a quality map. A producer well perforated 30m above OWC was fixed while a single injector perforated on all water layers varied its position. The final map was the cumulative production due to the pair of wells. Several maps of this kind were created and a mean value of 5MM m3 was obtained for both blocks. Figure 7-3: Cumulative production quality map with a fixed producer and variable injector position shows one of these maps as example, where the circle represents the fixed producer position and the cell values the cumulative production due to the injector placed on that position.

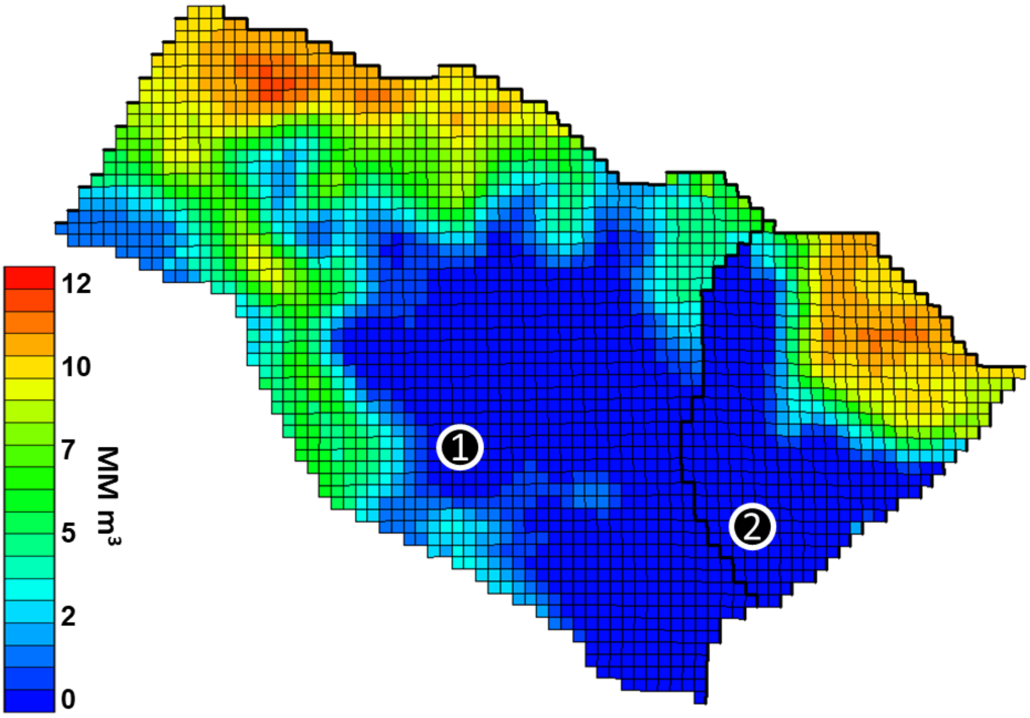

Figure 7-3: Cumulative production quality map with a fixed producer and variable injector position

Using the values of Np and RF obtained and the VOIP of the model we estimated an initial number of producers using EQB1, that is shown in Table 7-3: Estimative Number of Initial Well Producers.

Table 7-3: Estimative Number of Initial Well Producers

	High Block	Low Block	Mean
Number of Producers	10	3	13
Uncertainty	+-6	+-2	+-8

Initially the number of injectors were defined as a 1:1 ratio. The initial producer positions were determined using the quality map of Figure 5-5b, and the injectors positions were placed according to the quality map of Figure 7-3. The initial strategy obtained is shown on Figure 7-4 over a static map that is the sum of the product of the porosity, height and oil saturation ($h.\phi.S_o$) of all projected cells, on the final date of the project. We can observe in the Figure 7-4 that there is a non-drained region with remaining oil. That issue will be solved in the next optimization steps.

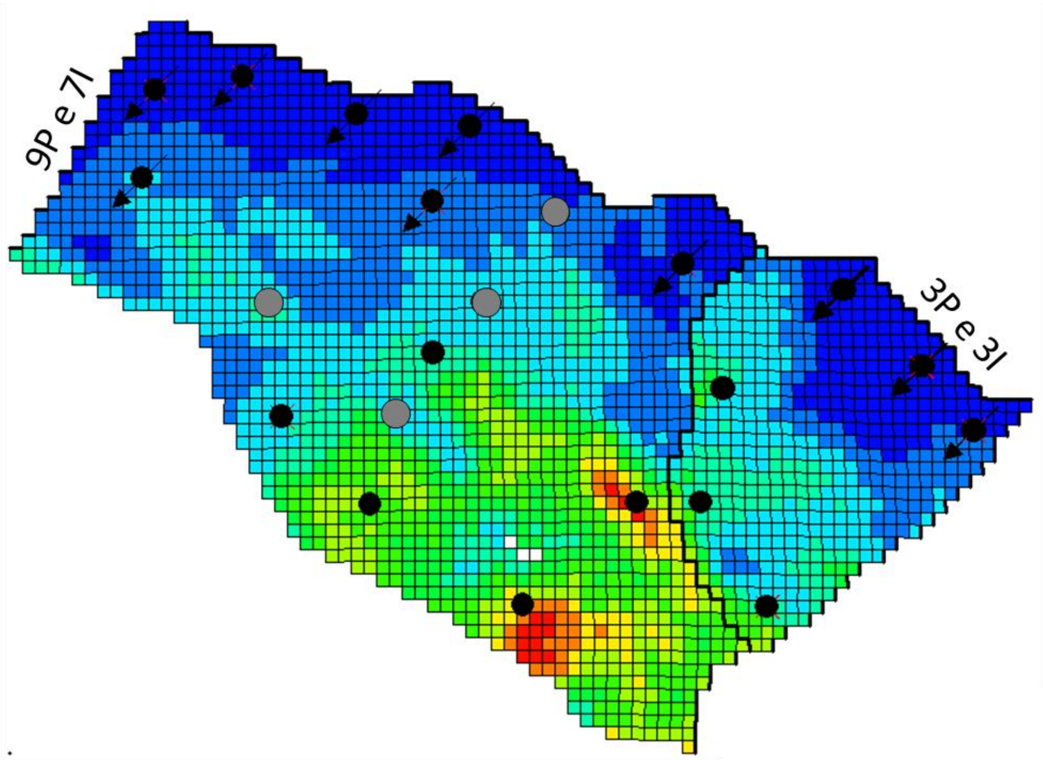

Figure 7-4: Initial production strategy model over the $h.\phi.S_o$ map in m^3.

APPENDIX B3: Well Number Optimization

We followed the hierarchical optimization presented in Figure 3-6. The objective function is the NPV, and the economic and well controls parameters were defined according to the benchmark case study (Gaspar *et al.*, 2023b). Table 7-4 shows the selected standard platform utilized and the correspondent processing capabilities for liquid and water rate, as well as water injection. During the optimization steps it was chosen to use a no flow limit condition until platform size optimization. That implied on a platform size of 2.04 times the values of Table 7-4.

Table 7-4: Standard Platform Processing Capacities

Liquid Flow Rate	Water Flow Rate	Water Injection
100.000 bpd/d	60.000 bpd/d	150.000 bpd/d

The first step is optimizing the number of wells. In this particular case the objective function is called FEI (field economic indicator) because the well schedule is not defined yet. This process was done manually, removing and adding wells and observing the variation on the FEI function. A total of nine simulations was run, keeping the total number of wells in a range of 20 to 24. Table 7-5 summarizes the results for wells number before and after the optimization.

Table 7-5: Well number optimization

	Nº Prod.	Nº Inj.	Iplat (Bi. USD)	FEI (Bi. USD)	RF (%)
Base Case	12	10	1.165	1.265	41.8
Nº Wells	11	12	1.165	2.452	56.4

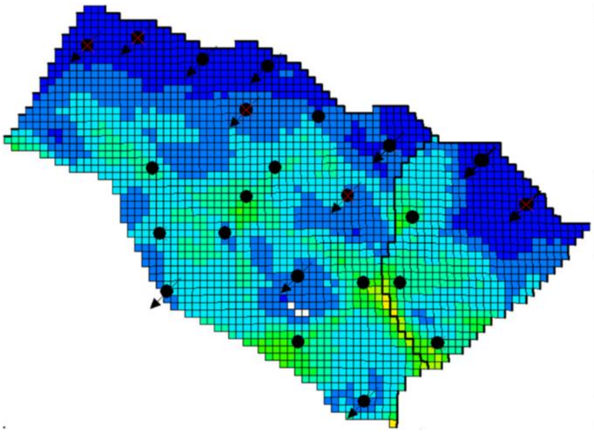

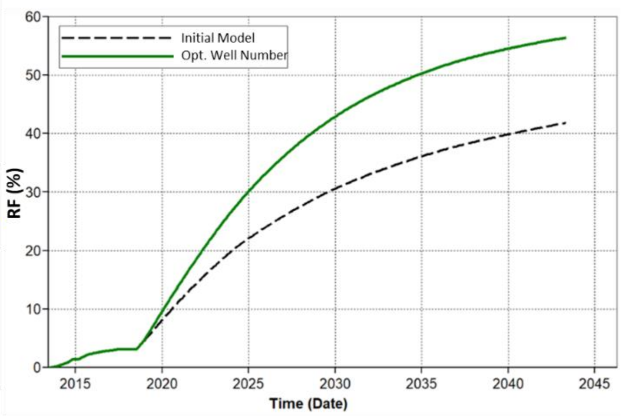

Figure 7-5: Final results obtained for (a) well number after optimization over the h.phi.so map (m3) and (b) recovery factor before (dashed) and after (continuous) optimization

APPENDIX B4: Well Position Optimization

An initial open schedule was defined following a decrescent Producer Well Economic Indicator (PWEI) order for producers and a crescent Injector Well Economic Indicator (IWEI) order for injectors (Ravagnani *et al.*, 2011). Wells were opened alternating between producers and injectors. We started with the high block, prioritizing the injectors at the north border. The proposed schedule resulted on a NPV of 2.118 Bi. USD and a RF of 55.8%.

Well position optimization was done without redoing the perforations, and with the following methodology: The spatial search of each well was restricted on its Voronoi region, as illustrated in Figure 7-6.

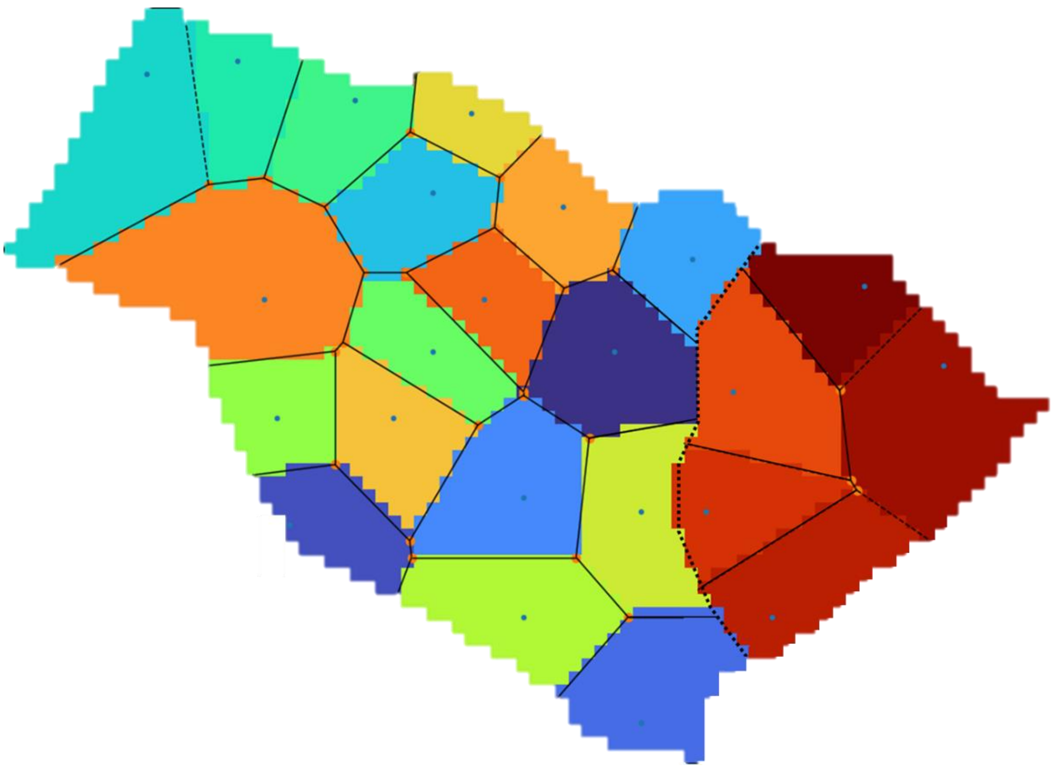

Figure 7-6: Voronoi regions for each well for the position optimization

The number of searches on each region was defined as 1 on each 3x3 block, in a way they were equidistant (Figure 7-7). The optimization process randomly selects a Voronoi region, and varies the well position within that region by fixing it on the highest NPV. The process continues by selecting a new region, until there is none left. Four wells (NA1A, NA2, NA3D and RJS19) were excluded from the optimization process as they was already drilled.

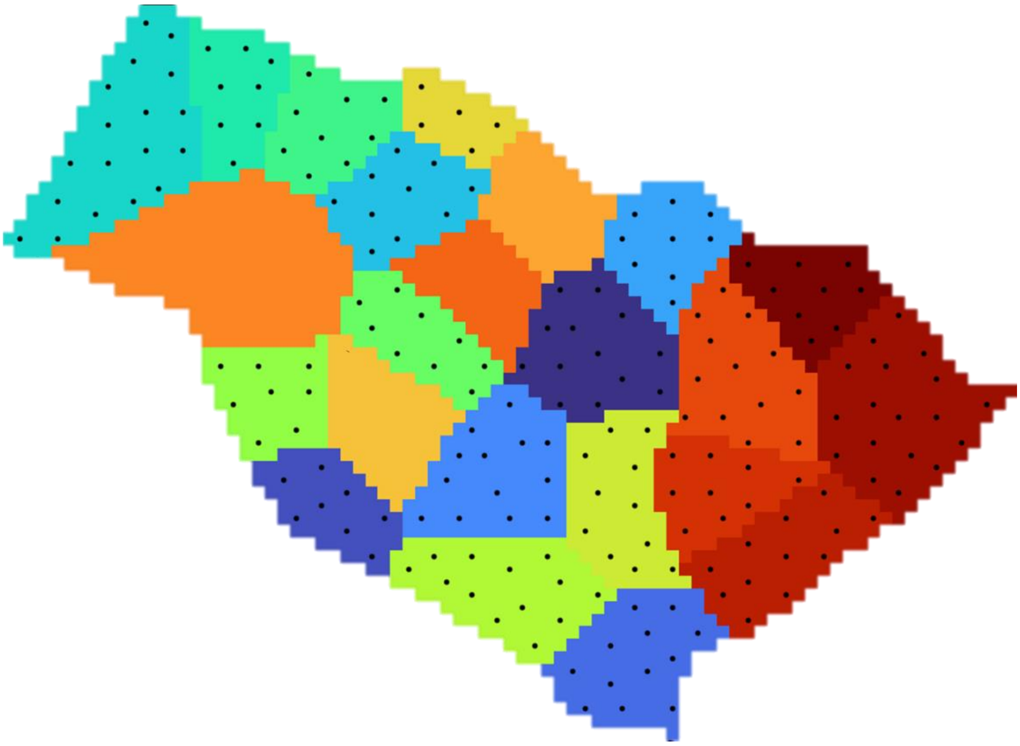

Figure 7-7: Well position search space for each Voronoi region.

Figure 7-8a shows the h.ϕ.S_o map with the optimized well positions, and Figure 7-8b the RF before and after the optimization. Table 7-6 summarizes the results obtained in this step.

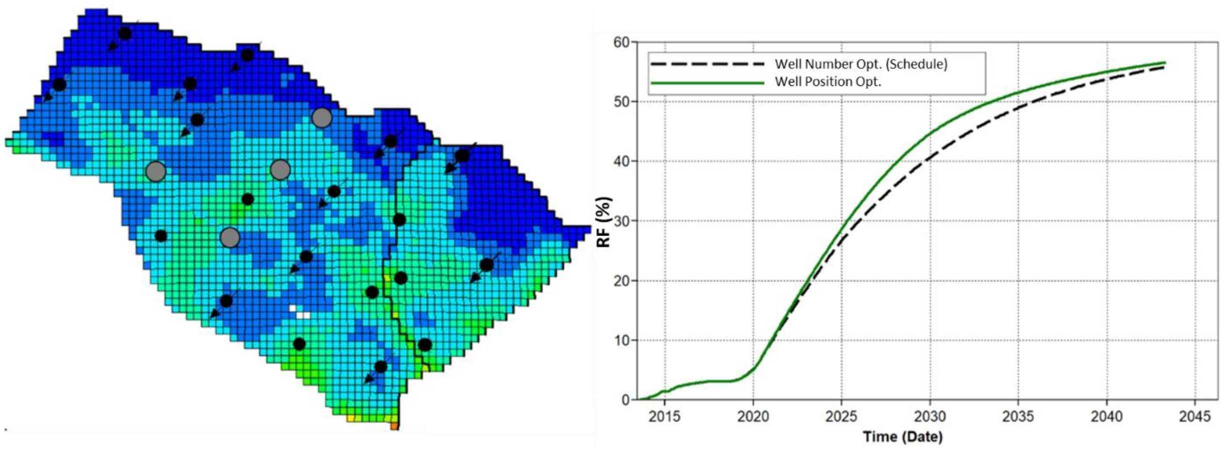

Figure 7-8:Final results obtained for (a) well positions after optimization over the h.phi.so map (m3) and (b) recovery factor before (dashed) and after (continuous) optimization

Table 7-6: Well Position Optimization Summary Results

	NPV (Bi. USD)	RF (%)	Nº Simulations	NPV increment (%)
Initial Schedule	2.118	55.8	-	-
Well Position	2.347	56.6	257	10.8

APPENDIX B5: Platform Limit Optimization

The platform limit optimization was done using a step of 5% between a 50% to 205% range of the model given on Table 7-4. In total 32 simulations were done improving the NPV from 2.347 Bi. USD to 2.633 Bi. USD with a final RF of 55.8% and a platform capacity of 115%. Figure 7-9a we have the NPV variation with the platform limit and Figure 7-9b the RF and the water production rate before and after the optimization.

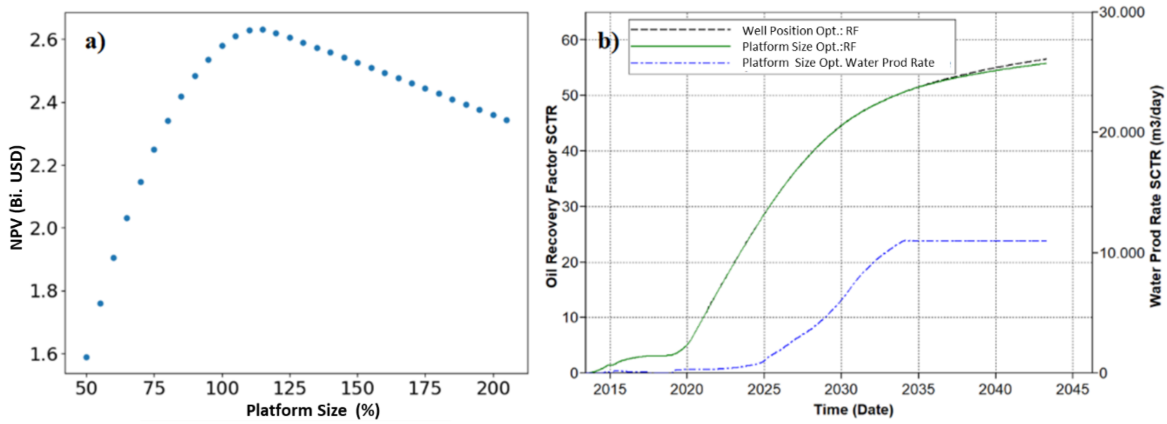

Figure 7-9: Platform size optimization results for (a) NPV variation with its standard size defined on table X and (b) recovery factor and total water production rate before (dashed) and after (continuous) the optimization.

APPENDIX B6: Well Schedule Optimization

Well schedule optimization was done considering 6 scenarios varying the well opening order by crescent or decrescent PWEI and IWEI, and starting by the high block or low block. Producers and Injectors were opened alternately. The best result was attained by the scenario C2, where we started the production by the low block with decrescent PWEI as showed on Table 7-7.

Table 7-7: Well Schedule Optimization Results

Scenario	C1	C2	C3	C4	C5	C6
NPV (Bi. USD)	2.695	2.713	2.702	2.643	2.614	2.632

**C1 – Decreasing PWEI starting from the high block. C2 – Decreasing PWEI starting from the low block. C3 – Decreasing PWEI considering both blocks. C4 – Increasing PWEI considering both blocks. C5 – Increasing PWEI starting from the high block. C6 – Increasing PWEI starting from the low block.*

Figure 7-10 shows the recovery factor before and after the optimization. Its values maintained at 55.8%. NPV increase happened because of oil anticipation.

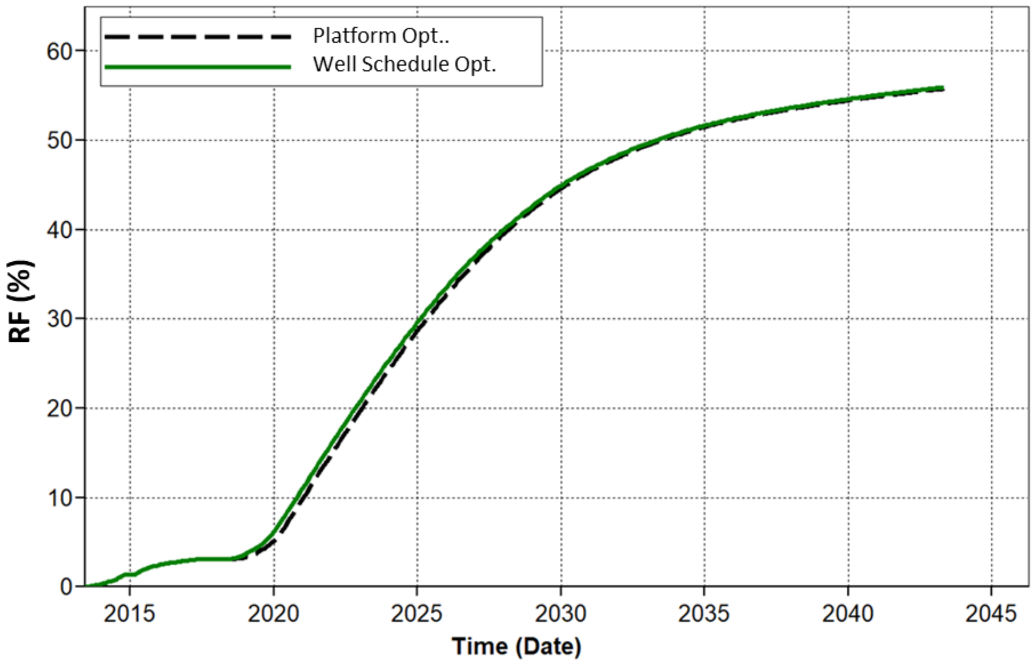

Figure 7-10: Recovery factor before (dashed) and after (continuous) the schedule optimization

APPENDIX B7: Well Shut in Optimization

Producers shut-in optimization was based on water cut. It was used the same BSW constrain for all wells with a 5% step from 75% to 100%. Figure 7-11 shows the RF variation with time before and after the optimization. The best water cut obtained was at 90%, as showed on Table 7-8: Water Cut Optimization.

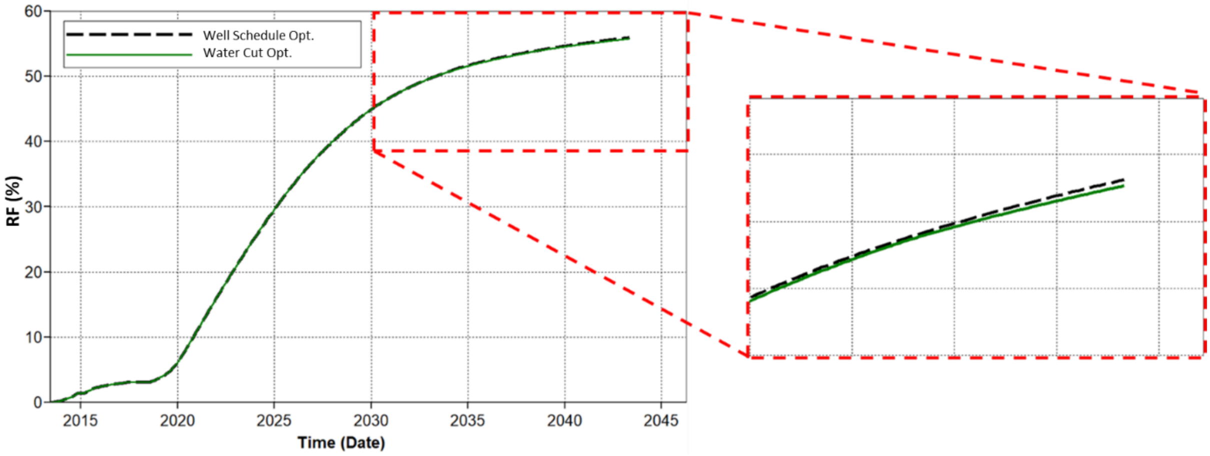

Figure 7-11: Recovery factor before (dashed) and after (continuous) the water cur optimization with a detail view at the end of the production.

Table 7-8: Water Cut Optimization

Water Cut (%)	75	80	85	90	95	100
NPV (Bi. USD)	2.656	2.683	2.708	2.723	2.718	2.713

APPENDIX B8: Optimization Results Summary Compilation

The strategy optimization followed a hierarchical approach with only one cycle. We started from a initial strategy after the history matched model. It was performed a well number, well position, platform size, opening schedule and shut-in optimization. Figure 7-12 summarizes the NPV and RF obtained on each step made.

Because the initial strategy had a drainage failure, the number of wells had the major impact on the NPV with a 93.8% variation. Platform size and well position are the other two most important variables on this reservoir strategy optimization, with respectively a 12.2% and 10.8% NPV change. The total number of simulations to achieve the final NPV was 269 with well position being the most demanded. Figure 7-13 shows the NPV variation with simulations runs, starting when the initial schedule was defined.

hithi

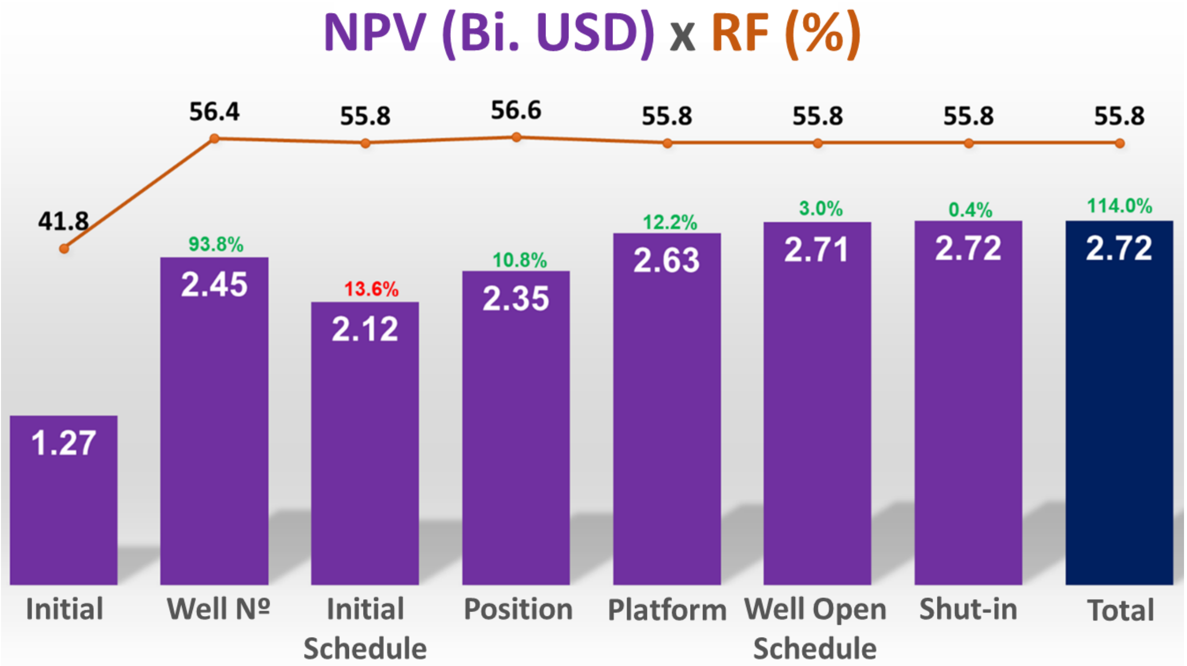

Figure 7-12: NPV and RF summary variation at each optimization step

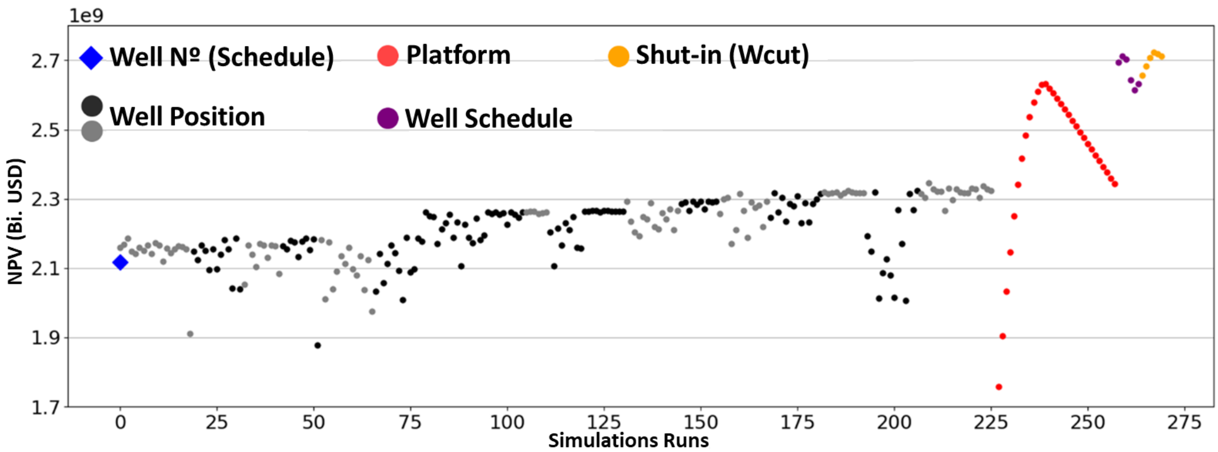

Figure 7-13: NPV versus simulations for each optimization step.